Open Access
Original paper

Budownictwo i Architektura / Civil and Architectural Engineering 25(3) (2026) 26044
https://doi.org/10.35784/bud-arch.8898

Holistic assessment of building behaviour in severe earthquakes: integrating ground response with structural dynamics and ground motion assessment

Lindung Zalbuin Mase[1,*], Aza Shelina[2], Aminah Rahmadani Lubis[3], Defina Yuandita[4], Jiratchaya Ayawanna[5], Salisa Chaiyaput[6]

[1] *Department of Civil Engineering, Faculty of Engineering, University of Bengkulu, Bengkulu, 38371 Indonesia; lmase@unib.ac.id*
[2] *Department of Civil Engineering, School of Engineering, King Mongkut's Institute of Technology Ladkrabang, Bangkok, Bangkok, 10520, Thailand; 67016001@kmitl.ac.th*
[3] *Department of Civil Engineering, Faculty of Engineering, University of Bengkulu, Bengkulu, 38371 Indonesia; g1b021039.aminahlubis@mhs.unib.ac.id*
[4] *Department of Civil Engineering, Faculty of Engineering, University of Bengkulu, Bengkulu, 38371 Indonesia; g1b021044.defina@mhs.unib.ac.id*
[5] *School of Ceramic Engineering, Institute of Engineering, Suranaree University of Technology, Nakhon Ratchasima, 30000, Thailand; jiratchaya@sut.ac.th*
[6] *Department of Civil Engineering, School of Engineering, King Mongkut's Institute of Technology Ladkrabang, Bangkok, 10520, Thailand; salisa.ch@kmitl.ac.th*

[*] *Corresponding Author*
Received: 20.12.2025; Revised: 03.07.2026; Accepted: 16.07.2026; Available online: 15.09.2026

Abstract:
This study analyses the Moot Court at the University of Bengkulu, Indonesia. The seismic ground response analysis and dynamic analysis are performed. The ground-motion parameters and the intensity of ground shaking are also discussed. The distribution of internal forces and stress ratio is presented. The identification of the weak structure and the retrofitting solution is analysed. The results show that ground-motion amplification can occur, potentially increasing peak ground acceleration by a factor of 1.684. The intensity parameters also indicate that ground surface motion has greater potential for seismic damage than at the pile-tip layers. Several beams are identified as weak structures. Retrofitting is carried out to overcome weaknesses in structural elements using the concrete jacketing method. The increase in cross-sectional area of the weakened beam is 52%, 47%, and 53% compared to the previous beam dimensions, and adding reinforcement could be effective in optimising overall structure performance.

Keywords:
seismic response analysis; dynamic analysis; structure inspection; retrofitting; concrete jacketing

1. Introduction

Bengkulu City is a coastal city on the island of Sumatra. The town of Bengkulu is an active seismic zone, attributable to its geographic position near the intersection of the Indo-Australian and Eurasian plates [1]. The location of Bengkulu City results in a high earthquake intensity [2]. The Bengkulu-Enggano and Bengkulu-Mentawai Earthquakes were caused by tectonic plate activity in the subduction zone [3]. A study by [4] reported that the Bengkulu-Mentawai earthquake occurred on September 12, 2007, with a magnitude of Mw 8.6, the largest earthquake in Bengkulu City in the last two decades. Mase [5] reported that the earthquake also caused extensive damage to buildings and the ground. Previous studies by Mase [5,6] identified the Mw 8.6 Bengkulu–Mentawai earthquake as the most credible seismic scenario for Bengkulu due to its high seismic hazard potential. Therefore, seismic hazard should be explicitly considered in the structural design of buildings in Bengkulu City.

Vibrations induced by ground motion during earthquakes can cause deformation and dynamic forces in building structures, leading to structural failure [6]. Therefore, this study evaluates the structural performance of the building under the expected loading from a large earthquake. The University of Bengkulu is the largest educational institution in Bengkulu Province. The university was established in April 1982, and numerous developments in its structural infrastructure have occurred since then. As noted in the previous paragraph, the university was also affected by a more severe earthquake in 2007. Infrastructure development has increased significantly over the past decade. There is a monumental building known as the Moot Court Building. The building was constructed in 2017. This building is a learning laboratory for students at the Faculty of Law, University of Bengkulu. Since 2007, a large earthquake has not reoccurred. Therefore, inspecting the building's performance is crucial, especially if a similar large earthquake were to occur again. Inspection of the building's performance during an earthquake is also essential for assessing the existing building's earthquake durability, thereby enabling appropriate measures to improve building performance.

One-dimensional seismic ground response analysis is a method used to simulate seismic wave propagation and observe soil behaviour and response [7,8]. Implementing this method could affect the frequency content and time history of each soil layer. For example, the process can produce the spectral acceleration and the acceleration time history, both of which are geotechnically important parameters in earthquake engineering. Structural dynamic analysis was performed to evaluate the building's response to seismic loading generated by the input ground motion at the foundation level [9]. In general, seismic ground response and structural dynamic analyses are conducted to observe material response under seismic excitation [10]. At the same time, the combination of the two methods is effectively used to assess soil-structure performance. The seismic ground response can be expressed in terms of spectral acceleration and acceleration time history, which are subsequently used as input motion for structural dynamics analysis. The implementation of this method remains rare, underscoring the uniqueness and innovation of this research. Furthermore, the predicted ground-motion characteristics from the seismic hazard assessment were used as input to the seismic ground-response analysis [11].

The seismic design code SNI 1726:2019 [12] is a crucial regulatory tool for Bengkulu City, a high-seismic area. This updated version of SNI 1726:2012 [13] is based on a probabilistic approach and is designed to ensure the safety and resilience of buildings in high-seismic areas. Mase [14] suggests that past events can serve as a reference for structural design in high-seismic-activity areas, further emphasising the importance of adhering to the seismic design code. It is not just a set of rules but a necessary tool for ensuring the safety and resilience of buildings in high-seismic areas.

This paper presents the implementation of an integrated method for seismic and structural dynamics analysis to assess the performance of the Moot Court Building at the University of Bengkulu. The deterministic hazard results from Mase [15] are used as a reference to determine the maximum credible earthquake. The maximum-credible earthquake input motion is applied to simulate seismic wave propagation. The motion at the tip resistance of the bore pile is used as the input motion for structural dynamics analysis. A structural dynamics analysis inspects the distribution of internal forces and stress ratios. The weak structure is then observed, and retrofitting is proposed to improve it. The integrated method proposed in this study significantly enhances building performance during earthquakes, offering promise for improved safety and reduced damage. The potential impact of this research, which could inspire the audience, particularly civil engineering researchers, practitioners, and students, to further explore and implement these findings in their work, is significant and should not be underestimated.

2. Materials and methods

2.1. Seismotectonic settings and geological conditions

Figure 1 presents the seismotectonic settings of Bengkulu Province. Many active earthquake sources surround Bengkulu Province [14]. The Sumatra Subduction Zone is the first active tectonic region known to produce a large earthquake. The zone is the boundary between two large active plates, the Indo-Australian and Eurasian plates [14]. On the mainland of Sumatra Island, a significant active fault, the Great Sumatra Fault, crosses the Island. Three areas are segments of this great fault. They are the Ketahun, Musi Kepahiang, and Ulu Manna Segments. According to Sieh and Natawidjaja [16], these Fault segments could produce low- to moderate-magnitude earthquakes with relatively shallow focal depths. The two main seismotectonic zones that are different (not symmetrical) in this area consist of the Indian Ocean-Australian Plate Subduction Seismotectonic Zone and the Sumatra Active Fault Seismotectonic Zone [17]. These two main seismotectonic zones act as sources of earthquakes in the Bengkulu City area. Mase et al. [3] stated that the subduction zone at the boundary between the Eurasian and Indo-Australian Plates triggered the 2007 Bengkulu-Mentawai Earthquake. It is also found between the great Sumatra Fault and a back-thrust arc fault called the Mentawai Fault [18].

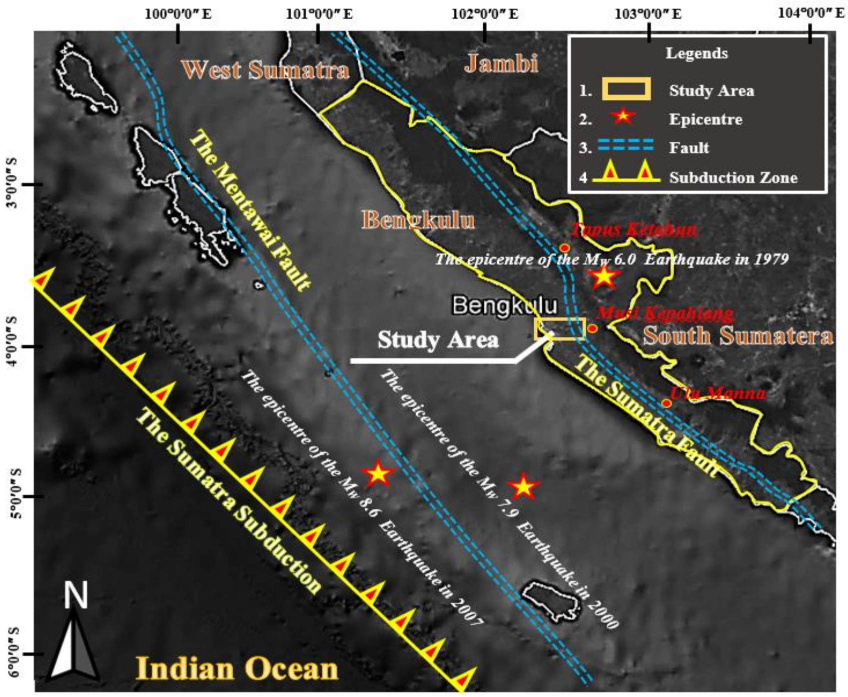

Fig. 1. Seismotectonic settings of Bengkulu Province (modified from [3])

Bengkulu is located in the fore-arc basin, known as the Bengkulu basin, consisting of sedimentary rocks and the oldest volcanoes [19,20]. Farid and Mase [21] suggested that one of the parameters influencing the level of damage caused by an earthquake is the local geological conditions. Bengkulu City has several types of geological formations, including alluvial terraces (Qat), Bintunan (QTb), swamp areas (Qs), reef limestone (QI), Andesite (Tpan), and Alluvium (Qa). The response of geological formations to seismic waves has different characteristics. Farid and Mase [21] stated that the dominant geological formations in Bengkulu City are alluvium terraces (Qat) and alluvium (Qa). These formations generally comprise loosely sedimented materials, such as sandy soils. Mase et al. [3] noted two main site classifications in Bengkulu City: Site Class C and Site Class D. Site Class C is generally located in the eastern part of the city. In contrast, Site Class D is usually located in the western part of Bengkulu City.

2.2. Study area and site investigation data

The University of Bengkulu is one of the most developed institutions in Bengkulu City today. This is evident in the numerous new buildings constructed to support student learning activities. Some of them are monumental buildings at the University of Bengkulu and are also referred to as commemorative structures for the establishment of the University of Bengkulu. One of the buildings at The University of Bengkulu is the Moot Court Building. This building is a learning laboratory for students at the Faculty of Law, University of Bengkulu. The University of Bengkulu (Fig. 2), located close to the west coast of Bengkulu City, is situated in a geological formation dominated by alluvium [21]. The building was constructed in 2017 and designed in accordance with the previous national design code, SNI 1726:2012. It should be noted that since 2019, the latest edition of the national design code, SNI 1726:2019 [21], has been applied to structural design. The updated regulations should be adapted to ensure the serviceability of this monumental building.

Figure 3 shows the soil conditions at the study site, i.e., the location where the building was constructed. This study conducted a site investigation, including a standard penetration test (SPT) and measurements of shear wave velocity (V_s). In general, based on on-site investigation, a stiff layer, indicated by an N-SPT of 60 blows/ft, is typically found at a depth of 10 m. Clayey and sandy soils dominate the site. The characteristics of local soil conditions during site investigations are key factors in evaluating the potential for earthquake-induced liquefaction [66]. Based on shear-wave velocity measurements, V_s values generally increase with depth, consistent with penetration resistance. The time-averaged shear-wave velocity at a depth of 30 m (V_{s30}) is about 325 m/s. The Building Seismic Safety Council (BSSC) [22] categorises the site as Site Class D because V_{s30} ranges from 180 to 360 m/s. Hollender et al. [23] also mentioned that areas with Site Class D are relatively more vulnerable to seismic damage. This opinion is generally applicable to the study area, based on the report by Hausler and Anderson [24], who noted that seismic damage is also commonly observed in the Muara Bangkahulu District. The building's location in an earthquake-prone zone and in an alluvial formation causes it to experience significant seismic effects. This is also supported by a study conducted by Farid and Mase [21], which reported that the seismic vulnerability index in Muara Bangkahulu District is relatively high. The engineering bedrock surface is indicated by a layer with a velocity exceeding 760 m/s [25]. The V_s profile also shows that the engineering bedrock surface is found at a depth of 33.9 m. Studies by [62,63], and [64] indicate that Bengkulu is a region with a high level of seismic hazard, characterised by the potential for strong ground shaking and liquefaction. These findings emphasise the importance of conducting comprehensive seismic hazard assessments and structural performance evaluations. The study by [65] indicates that several areas in Bengkulu are predominantly underlain by Site Classes C and D, which exhibit a high potential for site amplification.

Recently, Mase et al. [18] suggested that, along the Muara Bangkahulu River floodplain, where the University of Bengkulu is located, the engineering bedrock is generally found at depths of 5-99 m below the ground surface. Both Viani [26] and Mase et al. [18] report a similar pattern in bedrock engineering in the study area. Information about the bedrock surface is essential for the next step of the analysis, i.e., one-dimensional seismic wave propagation. This is because the input motion is first applied at the ground surface. Recent studies by [68] and [69] indicate that comprehensive site investigations, soil response analysis, cyclic soil behaviour evaluation, and energy-based liquefaction assessment contribute to more reliable assessments of seismic hazard and structural performance under strong-earthquake conditions.

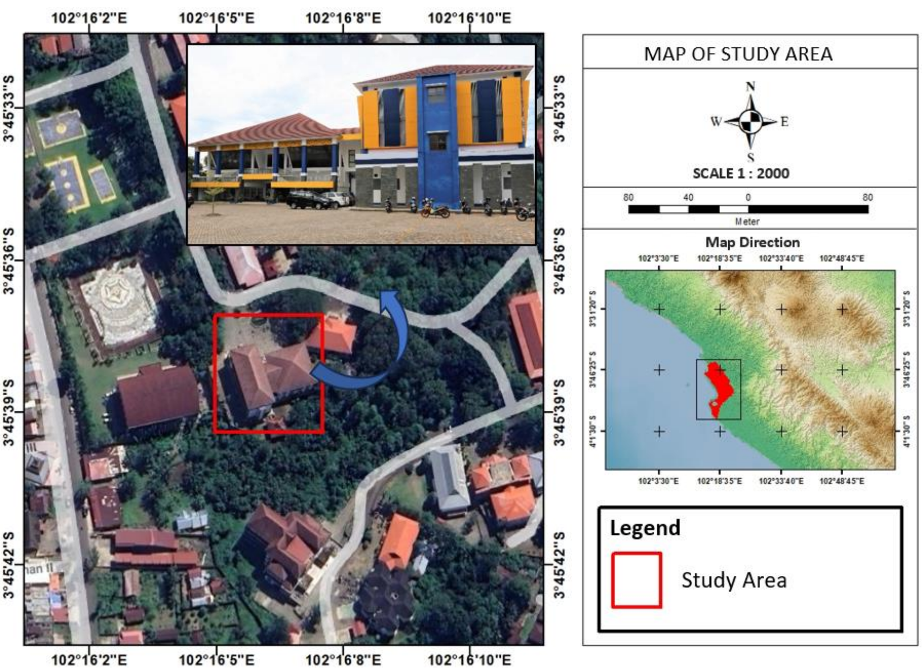

Fig. 2. The layout of the study area (source: own study)

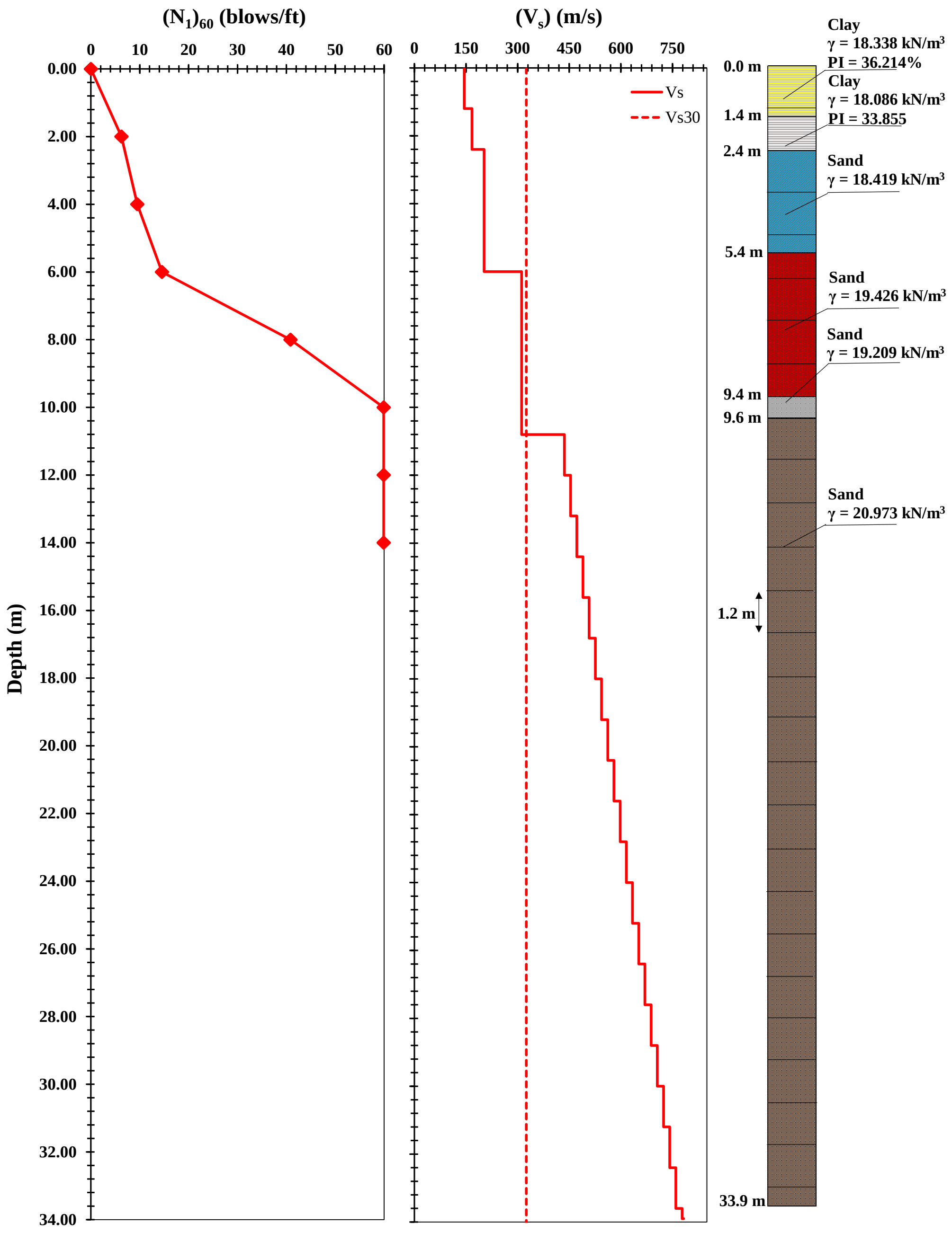

Fig. 3. Site investigation results and soil column model. Source: own study

2.3. Properties of the Moot Court Building

The University of Bengkulu Moot Court Building is located on the University of Bengkulu campus. The building, constructed in 2017, serves as the office of the Dean of the Faculty of Law at the University of Bengkulu. The Moot Court Building at The University of Bengkulu comprises two floors on the right side and three on the left. Each floor is 4 m high, with a total building height of 12 m. The first and second floors are used as learning activity rooms for students. The third floor is used as office space for employees. Figure 4 depicts the structural arrangement of various elements, including columns, beams, slabs, ring beams, and other floor plates. These structural elements are designed using a combination of frame and shell elements. The roof form is a truss roof, in which the roof load is distributed to the ring beam, which supports the trusses and the building's overall roof weight.

Table 1 lists the main structural components of the building for the analysis, including sloped columns, beams, floor plates, and beam rings. The bored pile foundation type is used to support buildings. The bore pile tip resistance is installed at a depth of 9.4 m below the ground surface. The concrete material used has the same compressive strength for all structural elements, namely 21 MPa. It is assumed that the bore pile foundation acts as an elastic support (spring), and both the bore pile and pile cap foundations are connected using point springs. Since the building is supported on bored-pile foundations tailored to site-specific soil conditions, the dynamic behaviour of the underlying soil plays an important role in modifying the earthquake ground motions transmitted to the structure. Therefore, incorporating dynamic soil response analysis into the seismic evaluation is essential for accurately assessing the interaction between ground motion and structural behaviour, thereby yielding a more representative evaluation of the building's seismic performance. The integration of dynamic soil response analysis and seismic evaluation improves the reliability of seismic hazard assessment under strong-ground-motion conditions [67].

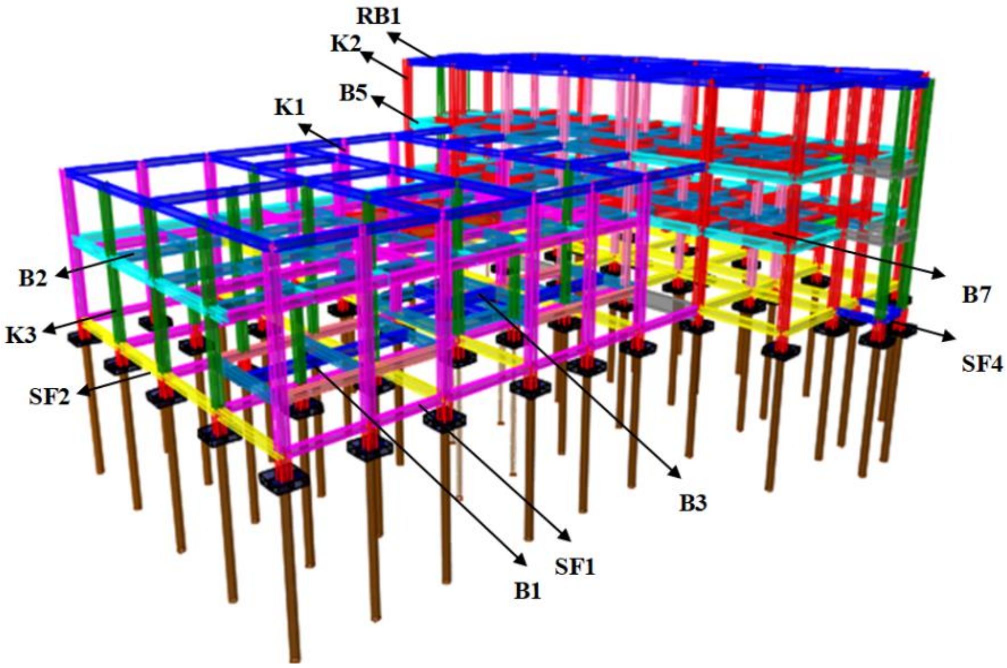

Fig. 4. 3D modelling of Moot Court Building structures

Table 1. Data on building structure

No	Structural Element	Notation	Dimension (mm)	Thickness (mm)	Characteristic of concrete compression (fc′) (Mpa)
1	Bore pile	BP	400	-	21
2	Sloop	SF1	250 × 400	-	21
		SF2	250 × 500		21
		SF3	150 × 1000		21
		SF4	200 × 300		21
3	Column	K1	400 × 500	-	21
		K2	450 × 450	-	21
		K3	400 × 400		21
4	Beam	B1	300 × 400	-	21
		B2	300 × 500		21
		B3	300 × 500		21
		B4	200 × 350		21
		B5	250 × 500		21
		B6	300 × 750		21
		B7	250 × 450		21
		B8	300 × 450		21
		B9	150 × 500		21
5	Beam Ring	RB1	150 × 400	-	21
		RB2	150 × 550		21
6	Platform	-	-	125	21

Specific location response and structural analyses were conducted in this research to assess the reliability of buildings at the study site. Figure 5 presents the synthetic waves from the 2007 Bengkulu-Mentawai earthquake, which are used as input waves for the analysis of earthquake wave propagation, based on the study by Mase [27]. As shown in Fig. 5, the maximum acceleration during the earthquake is 0.154 g. The characteristics of seismic waves can be predicted from site response analysis by propagating waves from the bedrock to the ground surface. The ground response is characterised by ground-motion parameters derived from seismic wave propagation analyses.

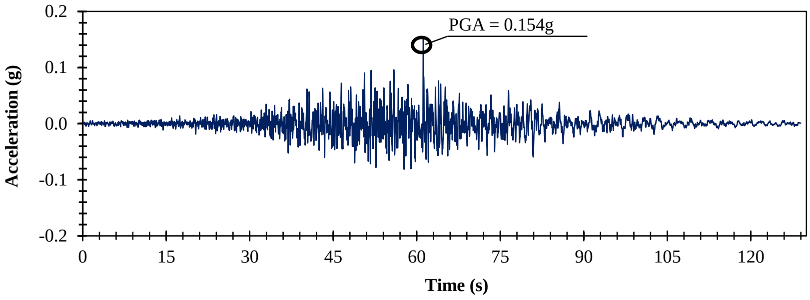

Fig. 5. The Mw 8.6 Bengkulu-Mentawai Earthquake in 2007. Source: own study modified from [27]

2.4. Ground motion parameters

Ground-motion intensity was characterised using several seismic parameters. These parameters were calculated using SeismoSignal software (SeismoSoft), including the PGA/PGV ratio and selected intensity measures (IMs). Several parameters are examined, including maximum peak ground acceleration (PGA_{max}), velocity (PGV_{max}), and displacement (PGD_{max}). In addition, the time at which the maximum values occurred is presented. The ground-motion period is also studied.

The ratio of maximum velocity to acceleration is commonly used to estimate the characteristics of the motion base. In terms of root-mean-square variables for the time-history component of ground motions, the formulations for root-mean-square acceleration, velocity, and displacement are generally mathematical, and the ratio of maximum velocity to acceleration is defined as.

$$a_{RMS} = \sqrt{\frac{1}{t_{tot}} \int_{0}^{t_{tot}} \left| a(t) \right|^2 dt} \tag{1}$$

$$V_{RMS} = \sqrt{\frac{1}{t_{tot}} \int_{0}^{t_{tot}} \left| v(t) \right|^2 dt} \tag{2}$$

$$D_{RMS} = \sqrt{\frac{1}{t_{tot}} \int_{0}^{t_{tot}} \left| d(t) \right|^2 dt} \tag{3}$$

$$\frac{v_{\max}}{a_{\max}} = \frac{\max\left|v(t)\right|}{\max\left|a(t)\right|} \tag{4}$$

where a_{RMS}, V_{RMS}, and D_{RMS} are root mean square values for acceleration, velocity and displacement, respectively. v_{max}/a_{max} is the ratio of maximum velocity to maximum acceleration. Spectrum Velocity and Spectrum Accelerations are also converted to spectrum intensity. Acceleration spectrum intensity (ASI), defined as the integral of the pseudospectral acceleration of a ground motion from 0.1 to 0.5 sec, was initially proposed as a ground-motion intensity measure relevant to the seismic response of the structure. The velocity spectrum of ground motion is the distribution of energy (or intensity) of seismic waves as a function of frequency, specifically the waves' velocity components. This spectrum provides valuable insights into how ground motion varies across frequencies, enabling the assessment of the potential impact of seismic events on structures and infrastructure. Sustained maximum acceleration (SMA) and sustained maximum velocity (SMV) are parameters that represent the sustained maximum acceleration/velocity over three cycles and are defined as the third-highest absolute value of acceleration/velocity in the time-history. The following equations give the formulations for determining ASI, VSI, SMA, and SMV.

$$ASI = \int_{0.1}^{0.5} S_a\left(\xi = 0.05, T\right) dT \tag{5}$$

$$VSI = \int_{0.1}^{0.5} S_V\left(\xi = 0.05, T\right) dT \tag{6}$$

The significant duration (SD), Arias Intensity (AI), and Cumulative Absolute Velocity (CAV) are also presented. SD is the interval over which a proportion (percentage) of AI is accumulated (the default is the interval between the 5% and 95% thresholds). AI is one of the most important parameters for characterising ground motion, as it can capture multiple characteristics simultaneously. Travasarou et al. [28] indicated that AI had been a suitable parameter for assessing damage, especially in short-period structures. Campbell and Bozorgnia [29] suggested that implementing CAV parameters across a wide range of engineering applications can indicate structural damage. They also introduced the Standardised Cumulative Absolute Velocity (Std-CAV). The formulations for these parameters are presented in the following equations,

$$S_D = \left| t_{AI=5\%} - t_{AI=95\%} \right| \tag{7}$$

$$AI = \frac{\pi}{2g} \int_{0}^{T_d} a(t)^2 \, dt \tag{8}$$

$$CAV = \int_{0}^{T_d} a(t) \, dt \tag{9}$$

$$Std-CAV = \sum_{i=1}^{N} \left(H\left(PGA_i - 0.025\right) \int_{i-1}^{i} \left| a(t) \right| dt \right) \tag{10}$$

$$H(x) = \begin{cases} 0, x < 1 \\ 1, x \geq 1 \end{cases} \tag{11}$$

Moreover, they are at the 5% and 95% thresholds of AI, respectively [28]. The a(t) is the absolute acceleration value at time t, and T_d is the total duration of the ground motion record, and g is the acceleration due to gravity. where N is the number of discrete 1-s time intervals, PGA_i is the value of the peak ground acceleration (g) in time interval i (inclusive of the first and last values), and H(x) is the Heavisine Step Function.

Several intensity parameters and frequency content, including Housner Intensity (HI), A_{95}, and Characteristic Intensity (I_c), are also crucial in ground motion analysis [30]. Housner Intensity is the spectrum intensity derived based on integrating pseudo-spectral velocity for the period range of 0.1 to 2.5 s. The A_{95} parameter has been proposed because PGA is often associated with high-frequency motions that have low energy and are challenging to predict. The A_{95} parameter is the acceleration level at which 95% of the arias' intensity is achieved. In the context of ground-motion parameters, I_c typically quantifies the overall intensity of ground shaking during an earthquake. It is usually tied to the magnitude of ground motion at a given location and to how that motion will likely affect structures and people. The formulation for HI and I_C is expressed in the following equations,

$$HI = \int_{0.01}^{2.5} PSV\left(\varepsilon = 0.05, t\right) dt \tag{12}$$

$$I_c = \left(a_{RMS}\right)^{\frac{3}{2}} \sqrt{t_{tot}} \tag{13}$$

$$A_{95} = 0.74 I_a^{\ 0.438} \tag{14}$$

where PSV is pseudo-spectral velocity and is the damping ratio of 5%.

The predominant period (T_0) is the period at which the most significant spectral acceleration occurs in the response spectrum at 5% damping. Elhout [30] suggested that the mean period (T_m) is the best-simplified frequency content characterisation parameter, being estimated with the following equation,

$$T_m = \frac{\sum C_i^2 / f_i}{\sum C_i^2} \tag{15}$$

where C_i are the Fourier amplitudes, and f_i represent the discrete Fourier transform frequencies between 0.25 and 20 Hz

The notion of adequate design acceleration (EDA), with various definitions, has been proposed by at least two researchers. High-frequency acceleration pulses induce little response in most structures. Effective Design Acceleration (EDA) is a practical design acceleration, defined as the peak acceleration after filtering out accelerations above 8–9 Hz. Gogoi et al. [31] suggested that the effective design acceleration be 25% greater than the third-highest (absolute) peak acceleration obtained from a filtered time history.

Maximum Incremental Velocity (MIV) is a ground-motion parameter used primarily in seismic engineering to characterise the velocity of a seismic event over time, specifically focusing on the maximum change in velocity during shaking. It is a valuable parameter for understanding how ground motion evolves and how rapidly ground velocity changes during an earthquake. This can have implications for structural design, as rapid changes in velocity can induce significant forces and vibrations that may compromise the integrity of buildings and infrastructure. The formulation of MIV is expressed in the following,

$$MIV = \max \left| \frac{dv(t)}{dt} \right| \tag{16}$$

where dv(t) is the change in velocity at a given time t, and dt is the time increment.

The Damage Index (DI) for ground-motion parameters is a key concept in structural engineering that quantifies the potential for structural damage due to seismic activity. The Damage Index measures structural performance in response to ground motion. Based on ground-motion parameters, it provides a means to assess the severity of an earthquake's effects on buildings and infrastructure. The Damage Index is used to assess the degree of damage a structure may sustain during an earthquake. It helps engineers evaluate structural resilience and identify seismic vulnerabilities of a building or structure under specified seismic loading conditions. The Damage Index is a dimensionless value that typically ranges from 0 (no damage) to 1 (total collapse or maximum expected damage).

The Number of Effective Cycles (NEC) is calculated as the summation of the ratios of the amplitudes of the cycles in the accelerogram divided by the maximum cycle amplitude and raised to the c exponent, determining the relative importance of different amplitude cycles, as proposed by Malhotra [32] and Hancock and Bommer [33]. The Impulsivity index (IP) indicates the ground motion's impulsive character. It is calculated as the developed length of the velocity time series divided by the Peak Ground Velocity, as detailed in the procedure of Panella et al. [34].

2.5. Research framework

This study follows the integrated framework proposed by Mase et al. [35], as shown in Fig. 6. Three primary analyses were conducted. The first is deterministic seismic hazard assessment, ground response, and structural dynamic analysis. The deterministic seismic hazard assessment is based on the previous study conducted by Mase [5,15]. Previous studies identified the Mw 8.6 Bengkulu–Mentawai earthquake as the most credible seismic scenario because it is associated with the highest predicted Peak Ground Acceleration (PGA) and the greatest potential damage intensity. Therefore, earthquakes should be considered in structural analysis and assessment. The following analysis simulates a one-dimensional seismic ground response analysis. One-dimensional nonlinear site-response analysis was employed to evaluate seismic wave propagation, assuming that the input ground motion originated at the engineering bedrock at each site [59]. The input ground motion corresponding to the most credible earthquake scenario was applied at the engineering bedrock surface.

The propagated wave at the pile tip (9.4 m deep) is collected. The wave is then used as the input motion for structural dynamic analysis. The final analysis involves simulating a structural dynamic analysis. This analysis aims to assess the building's structural performance and verify its safety. This integrated procedure enables a structural response that accounts for local conditions. By accounting for local conditions, the analysis results provide a more realistic assessment of the seismic demands acting on the building structure. Consequently, the influence of subsoil conditions, earthquake characteristics and the interaction between the structure and ground motion can be considered sequentially. In the dynamic structural analysis carried out to evaluate the dynamic response, the distribution of internal forces, displacements and the seismic performance of the building are based on ground motion derived from the soil response analysis. The results of this analysis are used to verify that the structure meets the required safety criteria and to assess its ability to withstand seismic loads in accordance with the selected earthquake scenario.

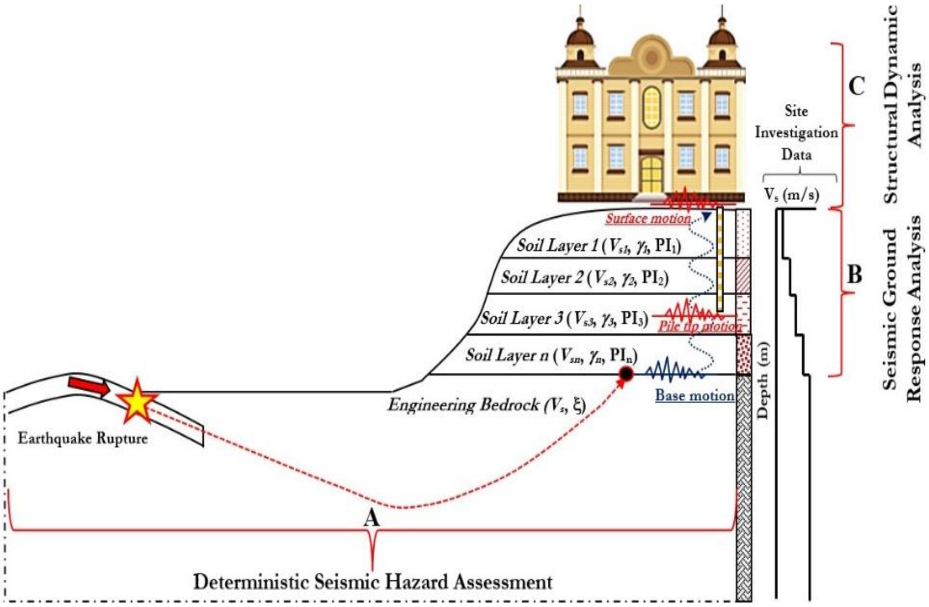

Fig. 6. The M_w 8.6 Bengkulu-Mentawai earthquake in 2007, modified from [35]

Figure 7 presents the detailed analytical framework implemented in this study. This study is initiated by collecting site investigation data, earthquake motion, and building information. The site investigation data includes the V_s profile, SPT-N Values, and soil profile. The earthquake motion is based on a study by Mase [27], as shown in Fig. 5. Based on the information provided in Fig. 3, the soil column is generated. To minimise the effect of high frequency during seismic ground response analysis, the wavelength analysis to estimate sublayer thickness is implemented based on the following equation,

$$d = \frac{V_s}{4 f_{max}} \tag{17}$$

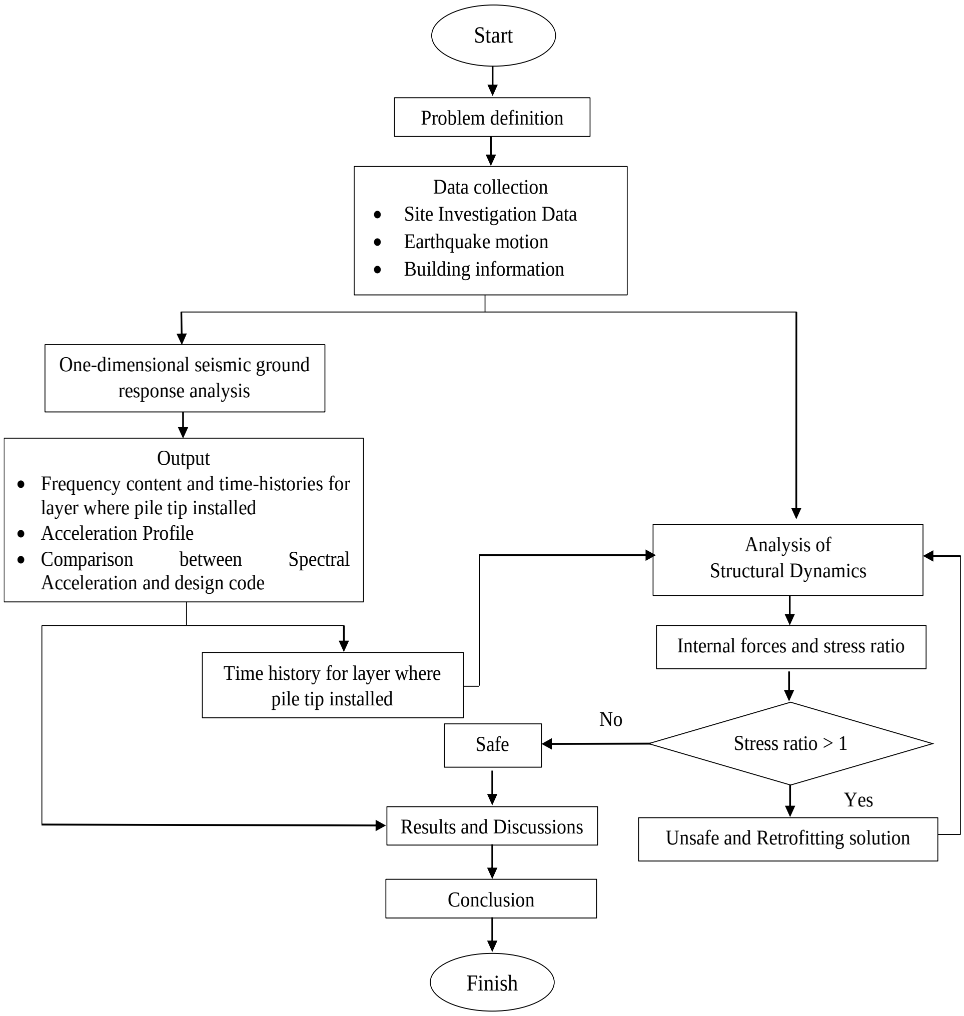

Fig. 7. Analytical research framework. Source: own study

In Eq. (1), d is soil thickness, V_s is the shear wave velocity (the minimum one), and f_{max} is the maximum frequency of 33 Hz. It should be noted that the thickness of each layer considered in this study, after calculation using Eq. (1), is 1.1 m – the plasticity index (PI) proposed by Fener et al. [36] can be obtained by correlating with V_p. Mase et al. [3] stated that the correlation between V_p and V_s can be used to determine V_p. For clayey soil, PI is estimated based on the following equations,

$$V_p = 1.25 V_s \quad (18)$$

$$PI = -16.49 \ln(V_p) + 121.95 \quad (19)$$

In Eqs. (2) and (3), V_p and V_s are the pressure wave and shear wave velocities, respectively.

Non-linear constitutive relationships are used to describe the hysteresis behaviour of soil during cyclic loading. The most straightforward constitutive model relates shear stress to shear strain, with the backbone curve represented by a hyperbolic function [37]. The modelled soil-structure interaction accounts for soil stiffness, with a damping ratio and boundary conditions consistent with the soil's dynamic characteristics, thereby realistically depicting the soil's dynamic behaviour. The Pressure-Dependent Hyperbolic (PDH) model is a non-linear constitutive model that extends the conventional hyperbolic model by accounting for the influence of effective pressure on the stress and strain behaviour of soil. This model describes changes in the shear modulus and strain characteristics at different levels. Some of the parameters used in this model are the damping ratio (ξ) and the shear modulus ratio (G/G_{max}), which are used to describe the degradation of stiffness and the dissipation of soil energy during cyclic loading. This model focuses on the hysteresis loop during cyclic loading and defines the backbone curve as a hyperbolic function. Seismic response modelling by propagating earthquake waves from the bedrock to the surface using the Pressure-Dependent Hyperbolic (PDH) model to obtain PGA values for each soil layer. A PGA is a measure of earthquake ground motion used as input in time-history analysis.

Table 2. Dynamic characteristics and attributes for response analysis, particular to a site

Layer Number	Layer Name	Depth (m)	Thickness (m)	V_s (m/s)	Density (kN/m^3)
1	Clay	1.2	1.2	144.911	18.338
2	Clay	2.4	1.2	167.196	18.086
3	Sand	3.6	1.2	202.351	18.419
4	Sand	4.8	1.2	202.351	18.183
5	Sand	6.0	1.2	311.507	19.566
6	Sand	7.2	1.2	311.507	19.426
7	Sand	8.4	1.2	311.507	19.309
8	Sand	9.6	1.2	311.507	19.209
9	Sand	10.8	1.2	435.859	20.336
10	Sand	12.0	1.2	453.866	20.404
11	Sand	13.2	1.2	471.874	20.475
12	Sand	14.4	1.2	489.882	20.546
13	Sand	15.6	1.2	507.890	20.618
14	Sand	16.8	1.2	525.897	20.691
15	Sand	18.0	1.2	543.905	20.762
16	Sand	19.2	1.2	561.913	20.833
17	Sand	20.4	1.2	579.920	20.904
18	Sand	21.6	1.2	597.928	20.973
19	Sand	22.8	1.2	615.936	21.041
20	Sand	24.0	1.2	633.943	21.109
21	Sand	25.2	1.2	651.951	21.175
22	Sand	26.4	1.2	669.959	21.240
23	Sand	27.6	1.2	687.967	21.304
24	Sand	28.8	1.2	705.974	21.367
25	Sand	30.0	1.2	723.982	21.429
26	Sand	31.2	1.2	741.989	21.490
27	Sand	32.4	1.2	759.997	21.549
28	Sand	33.6	1.2	778.005	21.608

Misliniyati et al. [38] stated that a non-linear, time domain-based analysis is commonly used for one-dimensional wave propagation problems. One-dimensional site response analysis is used to address the vertical propagation of horizontal shear waves through horizontally layered soil deposits [39]. The high level of seismicity in the study area necessitates evaluating seismic hazard and conducting site response analyses to support the design of earthquake-resistant structures [60]. A strain-dependent modulus reduction curve is used to define the backbone curve. Hashash et al. [40] developed one of the wave propagation models, namely the Pressure Dependent Hyperbolic (PDH) Model. Several curve-fitting parameters are suggested by

Hashash et al. [40]. The parameters b, s, and d for the soil model are derived from the recommendations of Hashash et al. [40]. Table 2 shows the soil physical parameter values used as input for soil modelling. The dynamic parameters of damping ratio (ξ) and shear modulus ratio (G/G_{max}) are based on reference curves. The curve from Vucetic & Dobry [41] is used for cohesive soil types by considering the PI value. Granular soil type using the curve from Seed & Idriss [42] under mean limit conditions, and does not consider PI. All parameters listed in Table 1 are then used in one-dimensional seismic ground-response analysis, as suggested by Mase et al. [35]. Combining seismic response analysis and structural analysis can be used to analyse building structures' resilience. Mase et al. [35] conducted research combining seismic response and structural analyses. One-dimensional wave propagation is used to determine the dynamic behaviour of soil layers during an earthquake. One-dimensional nonlinear site response analysis provides a more representative estimation of surface ground motion by accounting for the dynamic properties of soil layers [61].

Outputs such as the PGA profile, spectral acceleration, and time-history acceleration, especially at the layer where the pile tip is installed, are used for further analysis. To inspect the intensity parameter, the ground motion and intensity parameters at the pile tip, ground surface, and bedrock surface. Ground motion parameters, including frequency content and time histories, are observed. Those parameters include acceleration, velocity, and displacement. The spectral acceleration curve and the ratio of maximum velocity to maximum acceleration are also discussed. Several intensity parameters, including AI, SED, CAV, HI, MIV, NEC, and IP, are investigated to determine the potential seismic damage to the observed structure.

The following analysis in this research is a structural dynamic analysis based on the time history of acceleration, aimed at assessing structural reliability under earthquake loads. This analysis describes how a structure responds to ground motion over time during an earthquake. Structural loading refers to the Indonesian seismic design code SNI 1727:2013. The building structure loading values (load cases, load combinations, and mass sources) used are based on the authorised regulation in Indonesia, i.e., SNI 1727-2013 [43]. Time-history data from earthquake accelerograms are used to implement the University of Bengkulu Moot Court Building, which is modelled using the finite element method.

In the analysis, the bore pile foundation is assumed to act as an elastic support (spring), and both the bore pile and cap pile foundations are connected using point springs. The interaction between soil conditions and foundation structural elements is modelled using a rigid-wedged approach, enabling more accurate accounting for the impact of soil-structure interactions when evaluating structural capacity under earthquake loads. So, in analysing the interaction between foundation structural elements and the soil, it is assumed that this support interacts with the soil through springs. The soil that supports springs can withstand loads, and the modulus of subgrade reaction (k_s) from soil data influences this support. The vertical soil stiffness (K_{sv}) and horizontal soil stiffness (K_{sh}) values were obtained from Bowles [44]. Data regarding point spring values can be seen in Table 3. The formulations for vertical (K_{sv}) and horizontal (K_{sh}) modulus of subgrade reactions, as suggested by Bowles [44], are expressed in the following equations

$$K_{sv} = 40FS(Q_s) \tag{20}$$

$$K_{sh} = 2K_{sv} \tag{21}$$

where FS is the factor of safety (assumed to be 3 in engineering practice), and Q_s is the allowable bearing capacity of the bored pile.

In this study, the ultimate bearing capacity of the soil (Q_s) was obtained from the Aoki and Velosso [45] method. Analysis of the building model provides information on structural safety, displayed through colour differences in structural elements based on the stress ratio. The internal forces resulting from this research are the normal force (NF), the shear force (SF), and the bending moment (BM).

Unsafe structural elements are marked as over-strength elements. Unsafe elements are later analysed for repair methods using retrofitting in the form of concrete jacketing. It is a structural repair method that covers old concrete with new concrete to strengthen weak structural elements. Concrete jacketing [46,47] is a structural repair method that covers existing concrete with new concrete to strengthen weak structural elements. Furthermore, the dynamic analysis is reformulated to assess the building's performance after retrofitting treatment.

Table 3. Modulus of subgrade reaction value

Layer	Q_u (kN/m^2)	Q_a (kN/m^2)	k_{sv} (kN/m^3)	k_{sh} (kN/m^3)
Clay (layer 1)	441.670	176.668	21200.171	42400.342
Clay (layer 2)	460.512	184.205	22104.588	44209.175
Sand (layer 3)	811.968	324.787	38974.478	77948.957
Sand (layer 4)	769.444	307.778	36933.307	73866.614

3. Results and discussion

3.1. Peak ground acceleration profile

The seismic response analysis, a crucial component of this research, yields significant ground-motion parameters, including ground-amplification factors and spectral acceleration. Incorporating the input motion developed by Mase [27], the results of the seismic response analysis use a nonlinear approach in the form of PGA and spectral acceleration, providing valuable insights into the structural behaviour during seismic events.

The PGA value from the seismic response analysis results is shown in Fig. 8. PGA provides an overview of the area's seismic conditions. Figure 8 shows that the earthquake acceleration increases from the bedrock layer to the ground surface. The results revealed that the maximum earthquake acceleration occurred in the surface layer at 0.259 g. This layer consists of organic clay. This preconditioning of the organic clay layer triggers a relatively significant amplification effect during a strong earthquake. The results of this research reveal that the PGA value has relative stability. The amplification factor is obtained by comparing the peak ground motion (PGA) from the input motion with the PGA in the surface and foundation layers. The results show an amplification value of 1.684 for the surface layer and 1.000 (no amplification) for the foundation layer. The amplification factor refers to the increase in earthquake acceleration from the bedrock layer to the ground surface. This increase depends on the variation of Vs in each soil layer. When it reaches ground level, V_s decreases, increasing the amplification factor. The presence of clay soil can significantly amplify the ground surface response as a weak layer that controls the elastic response during earthquake shaking. Bedrock with high stiffness can produce a significant amplification factor [18,38]. This is caused by differences in V_s among soil layers. The smaller the Vs value, the greater the amplification factor value, such as the surface layer, which has a significant amplification factor and a small V_s value [48].

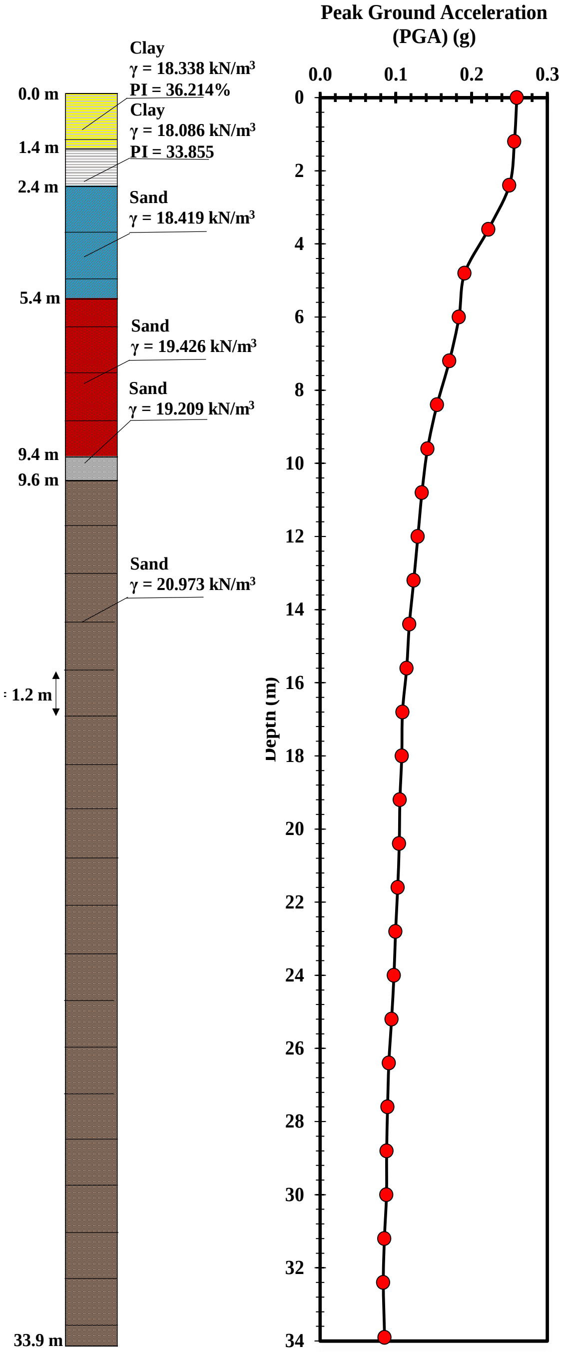

Fig. 8. PGA profiles from seismic ground-response analysis

3.2. Comparisons of the time history of acceleration and spectral acceleration

A comparison of ground motion time histories is shown in Fig. 9. This comparison is crucial, as it provides insights into the building's seismic response and helps evaluate its structural performance. In Figure 9, it can be observed that the PGA at the foundation layer (at the tip of the pile) remains the same as the input motion, whereas the ground-surface PGA is generally higher than the input motion. The calculation shows that the maximum PGAs at the ground surface and pile tip layer are 0.2598 g and 0.1543 g, respectively. For velocity, the maximum velocity is higher at the ground surface than at the pile-tip layer. The maximum velocities for those layers are 14.52 cm/s and 12.82 cm/s. For the displacement, the maximum values at the pile tip layer and the ground surface are also shown in Fig. 9, ranging from about 9.62 to 9.68 cm.

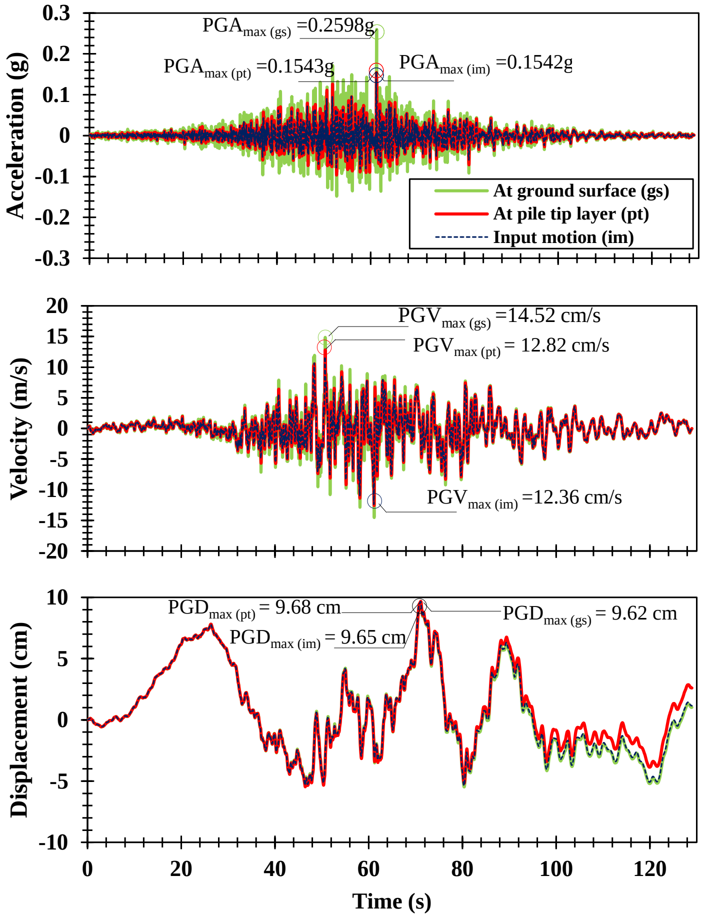

Fig. 9. The results of one-dimensional seismic ground response analysis for acceleration, velocity, and displacement

Figure 10 shows the comparison of spectral acceleration. Three spectral accelerations represent the surface soil layer (i.e., soft, medium, and stiff soil), the spectral acceleration at the layer where the pile tip is installed, and the spectral acceleration of the input motion. From this, it can be seen that the spectral acceleration value from the analysis tends to be lower than the results for SNI 1726:2019 in Bengkulu City. The results of this analysis also indicate that the building designed under the updated regulation can be considered relatively safe in the face of an earthquake, as the spectral acceleration value does not exceed the limits set by seismic design standards. The results also showed that the resonance effect may be significant within 0.2-0.3 s. Based on Mase et al. [49], a period of 0.2 s to 0.5 s corresponds to low- to medium-storey buildings, typically estimated as T = 0.1n (where n is the number of storeys). The analysis findings show that when the input waveform is applied, the spectral acceleration gradually increases in the period from 0.2 seconds to 0.4 seconds. The maximum spectral acceleration at the ground surface is 0.802 g at 0.253 seconds, and at the foundation it is 0.465 g at 0.345 seconds. The increase in spectra on the surface and foundation layers is due to spectral acceleration being influenced by soil density: denser soil yields smaller ground acceleration values.

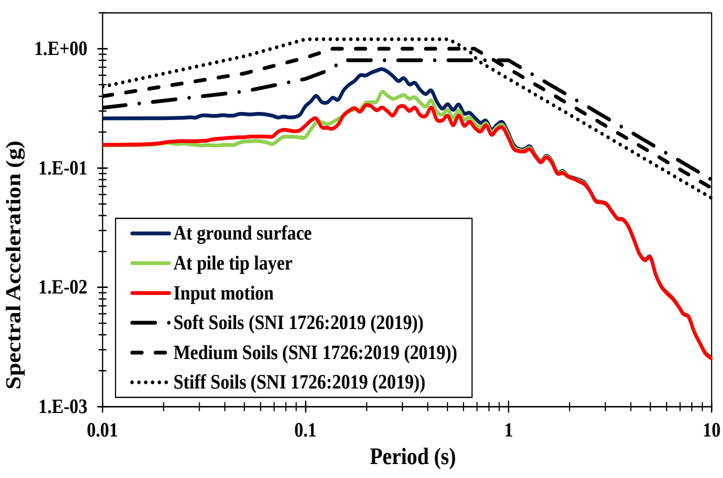

Fig. 10. Spectral acceleration comparison for spectral

3.3. Significant duration, arias intensity, and pulse velocity

Figure 11 shows the significant duration, Arias Intensity, energy flux and impulsive velocity for the input motion at the ground surface and the pile tip layer. The figure shows that the significant duration for the layer under consideration is generally between 44 and 48 seconds. It can also be concluded that during the 130-second shaking duration, about 34 to 37 shaking durations can significantly influence the site and structure response. Over this significant duration, the achievable pulse velocity is about 6.56 to 7.46 cm/s. At the ground surface, the pulse velocity during an earthquake is about 7.46 m/s, and at the pile tip layer, it is about 6.56 m/s. An extreme pulse velocity, i.e., more than 3 m/s, indicates high intensity and can significantly affect structures. Buildings and infrastructure in the affected area experience high demands, often leading to structural failure [50]. In this study, the Pulse Indicator (PI) for the input motion, motion at the pile tip layer, and motion at the ground surface generally ranges from 0.235 to 0.46, indicating no pulse-like behaviour. The pulse indicator is still below the threshold, i.e. 0.3 [51]. Understanding the non-pulse and pulse indicators is important in seismic hazard analysis and structural engineering.

The energy flux at the pile tip layer and the ground surface is a significant factor in understanding the force exerted on buildings and infrastructure during an earthquake. High energy flux means more force is exerted, increasing the likelihood of collapse. The combination of a long, significant duration, the pulse, and the energy flux could serve as an indicator of the possible impact of earthquake shaking on a building. In this study, at the pile tip layer, where the pulse indicator shows no pulse or in other words, the impact of the earthquake is not significant. However, inspecting the building response is still required to identify potential weak structures during seismic wave propagation.

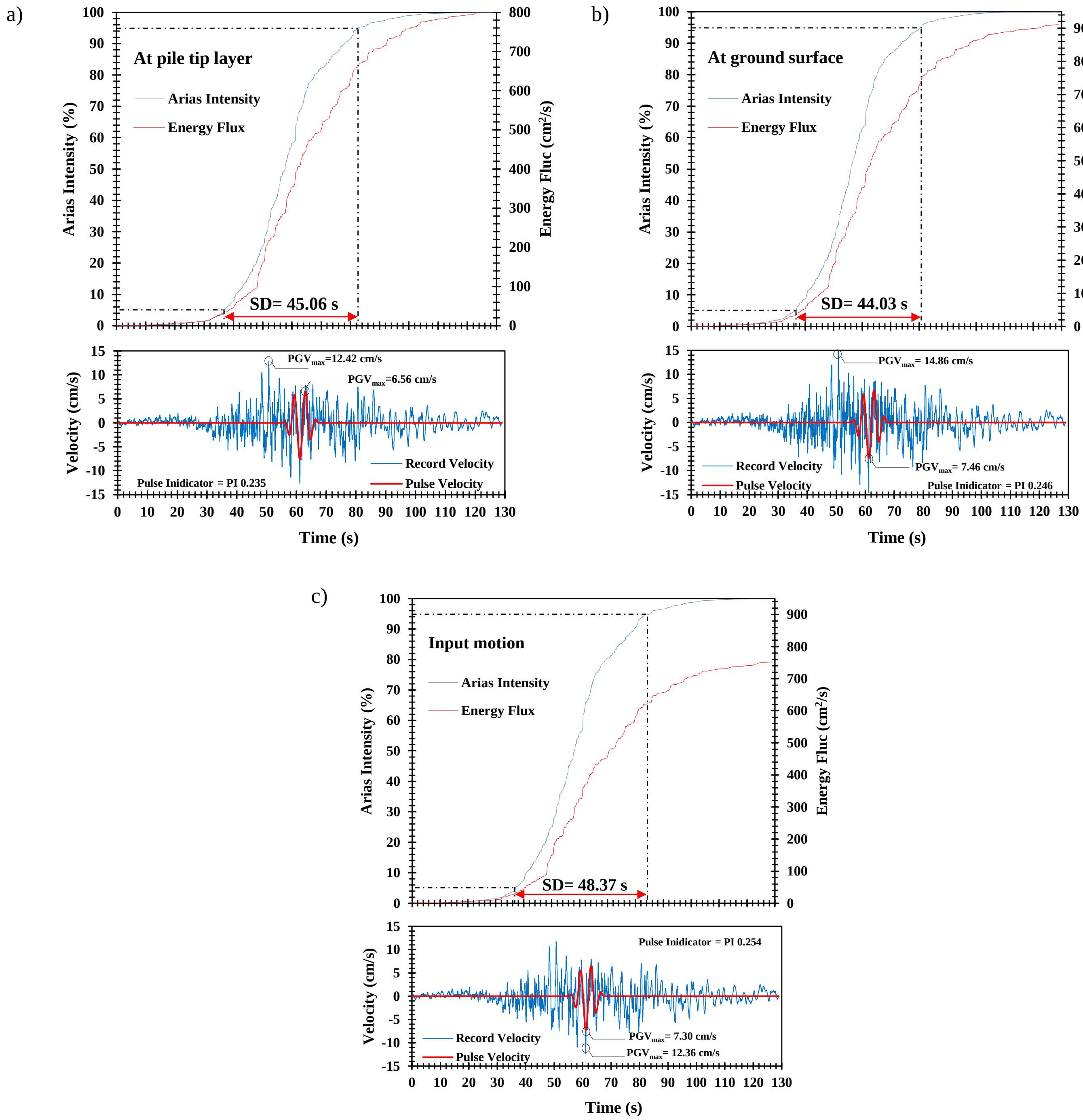

Fig. 11. Significant duration, Arias Intensity and Pulse Velocity for (a) input motion, (b) at the pile tip layer, (c) at the ground surface

3.4. Ground motion and intensity parameters comparison

Table 4 presents the ground motion parameters for the input motion, the propagated motion at the pile-tip layer, and at the ground surface. This study presents several intensity measurements, such as AI, Ic, SED, CAV, HI, DI, and IP. In general, the values of those intensity parameters are more significant at the ground surface.

Table 4. Ground motion parameters

Parameter	Input Motion	At the pile tip layer	At the ground surface	Unit
Max Peak Ground Acceleration (PGA_{max})	0.154	0.154	0.260	g
Time of PGA_{max}	61.170	61.240	61.280	s
Max Peak Ground Velocity (PGV_{max})	12.355	12.819	14.860	cm/s
Time of PGV_{max}	61.110	50.740	50.730	s
Max Peak Ground Displacement (PGD_{max})	9.653	9.676	9.619	cm
Time of PGD_{max}	71.090	71.130	71.150	s
PGV_{max}/PGA_{max}	0.082	0.085	0.058	s
Acceleration Root Mean Square (a_{RMS})	0.017	0.020	0.029	g
Velocity Root Mean Square (V_{RMS})	2.415	2.498	2.657	cm/s
Displacement Root Mean Square (D_{RMS})	3.558	3.475	3.569	cm
Arias Intensity (AI)	0.581	0.770	1.684	m/s
Characteristic Intensity (I_c)	0.025	0.031	0.056	-
Specific Energy Density (SED)	752.205	804.952	910.866	cm2/s
Cumulative Absolute Velocity (CAV)	1327.068	1511.915	2213.151	cm/s
Acceleration Spectrum Intensity (ASI)	0.114	0.133	0.192	g×s
Velocity Spectrum Intensity (VSI)	60.703	64.315	71.230	cm
Housner Intensity (HI)	58.164	60.713	64.922	cm
Sustained Maximum Acceleration (SMA)	0.095	0.111	0.149	g
Sustained Maximum Velocity (SMV)	10.960	11.379	12.855	cm/s
Effective Design Acceleration (EDA)	0.157	0.154	0.258	g
A_{95} parameter (g)	0.067	0.081	0.120	g
Predominant Period (T_0)	0.200	0.240	0.240	s
Mean Period (T_m)	0.630	0.568	0.391	s
Max Incremental Velocity (MIV)	17.319	19.477	22.146	cm/s
Damage Index (DI)	0.735	1.003	3.090	-
Number of Effective Cycles (NEC)	8.782	11.556	13.853	Cycles
Impulsive Index (IP)	108.741	119.062	148.540	-
Average Spectral Acceleration (SA_{avg})	0.142	0.149	0.167	g
Standardised CAV (Std-CAV)	0.674	0.859	1.599	g×s

AI for the considered ground motion ranges from 0.581 to 1.684 m/s. A larger AI indicates a more substantial level of ground shaking during an earthquake. In practical terms, a higher AI value suggests more severe shaking, which typically corresponds to a more significant potential for damage to structures and infrastructure [52]. It is primarily used in seismology to quantify the effects of an earthquake on buildings, structures, and the environment. For I_c, it can be observed that 0.025 to 0.056. A larger Characteristic Intensity (I_c) indicates a higher level of earthquake ground shaking that is likely to cause damage to structures [53]. For SED, the values range from 752.205 to 910.866 cm^2/s. A more significant SED implies a more powerful earthquake with potentially more significant consequences for the affected region [53]. For CAV, the values range from 1327.068 to 2213.151 cm/s.

A larger CAV indicates that the ground has undergone significant movement, both in the intensity of the shaking and in its duration. So, when the CAV is higher, the earthquake is more likely to cause significant damage and potentially pose a greater risk to people and buildings due to the sustained nature of the shaking [53]. HI for the considered ground motions generally varies from 58.164 to 64.922 cm. A more considerable HI value indicates an earthquake with the potential for substantial damage, emphasising the need for preparedness and earthquake-resistant infrastructure in the affected region. DI for the considered motions are observed to vary from 0.735 to 3.090. Generally, a larger DI indicates more severe seismic activity, leading to a greater potential for damage to buildings and infrastructure [54]. IP values for the considered motions vary from 108.741 to 148.540. A more extensive Impulsive Index of ground motion typically indicates that the seismic event has more sudden, sharp, or brief energy bursts [34]. This can lead to intense but short-lived shaking. In contrast to a more sustained or continuous shaking, impulsive ground motions are characterised by rapid, forceful movements that can cause localised damage, especially to structures less capable of absorbing such quick, intense forces.

Based on the results, the surface-layer ground-motion intensity parameters show the highest values. It is noted that a higher intensity parameter reflects the potential seismic damage the site may experience. In this study, the building foundations are located at a deeper layer, and there are no shallow foundations. However, the interface between the ground surface and the building could be an issue due to the seismic wave propagation. The effect of ground amplification at sites is also crucial. The soil improvement can be performed to minimise the intensity parameter. This is important for improving the material's shear modulus and damping ratio, thereby reducing ground-motion amplification.

3.5 Dynamic response of a building

The implementation of structural dynamic analysis based on finite element modelling in examining the behaviour of building structures involves observing the building's response to various types of loads, including dead loads, live loads, and earthquake loads. In modelling and structural analysis, it is necessary to evaluate the participation of various masses. According to SNI 1726:2019, structural analysis must consider various vibration modes that result in combined mass participation of 100% of the structure's total mass. However, an alternative analysis option allows the use of at least 90% of the sum of the combined vibration variations in each orthogonal horizontal direction of the analysed response. In this research series, the mass participation value was determined from 450 vibration variations (shape modes) to achieve a total mass participation of 100%, as summarised in Table 5. The first three vibration patterns are those with the most significant translation values, representing vibrations in the x-direction, y-direction, and rotation. Table 6 shows the maximum vibration variation pattern period in the building's x and y directions and rotation.

Figure 12 shows the results of the inspection of the concrete structure after structural analysis. The research showed that the building experienced structural failure in 12 elements. Structural failure can be assessed using the stress ratio parameter. The structural profile is safe if the stress ratio is less than 1; otherwise, it is unsafe. The stress ratio is a parameter that compares the internal force to the maximum strength a structural element can accept. Elements that show vulnerability are beams, for which finite element analysis indicates that some require special strengthening against shear loads. After structural analysis, the internal force values were obtained using the finite element method. Each structural element will produce internal forces because this building uses a rigidly interconnected floor system.

Table 5. Mode shape values in building structures for the first three mode shapes

Mode Shape	T (s)	UX (mm)	UY (mm)	RZ (mm)	SumUX	SumUY	SumRZ
1	0.805	0.004	0.522	0.279	0.004	0.522	0.279
2	0.741	0.803	0.004	0.000	0.806	0.526	0.279
3	0.614	0.001	0.264	0.486	0.807	0.790	0.766

Table 6. The value of internal force analysis

Code	Maximum internal forces before earthquake loads			Maximum internal forces after earthquake loads			Percentage increase (%)		
	Normal force (NF) (kN)	Shear force (SF) (kN)	Bending Moment (BM) (kNm)	Normal force (NF) (kN)	Shear force (SF) (kN)	Bending Moment (BM) (kNm)	Normal force (NF) (kN)	Shear force (SF) (kN)	Bending Moment (BM) (kNm)
B1	17.37	31.87	28.67	36.53	51.18	76.98	110	61	169
B2	62.51	106.37	135.72	156.97	212.76	230.72	151	100	70
B3	14.75	41.19	43.93	22.15	49.43	76.09	50	20	73
B4	2.14	12.46	10.73	2.59	16.20	15.36	21	30	43
B5	11.01	82.58	107.71	26.43	148.64	168.04	140	80	56
B6	18.74	120.03	159.01	24.35	144.09	227.38	30	20	43
B7	20.37	37.51	50.72	24.60	49.60	62.87	21	32	24
B8	4.89	27.01	42.86	5.51	38.50	56.16	13	43	31
B9	13.58	69.70	44.32	19.01	86.01	65.26	40	23	47
K1	457.72	30.59	53.53	732.28	39.55	91.17	60	29	70
K2	1150.66	70.78	142.51	1610.91	95.71	186.69	40	35	31
K3	619.28	96.93	70.19	867.96	130.36	94.29	40	34	34
K4	1031.84	37.39	71.05	1444.58	55.82	99.46	40	49	40
RB1	59.85	34.33	46.16	77.81	47.68	66.47	30	39	44
SF1	53.91	49.22	71.28	64.71	71.66	93.35	20	46	31
SF2	58.07	55.43	38.53	63.87	77.60	48.64	10	40	26
SF3	20.51	57.32	97.90	26.67	80.26	121.41	30	40	24
SF4	3.93	44.73	41.82	4.71	55.06	51.02	20	23	22

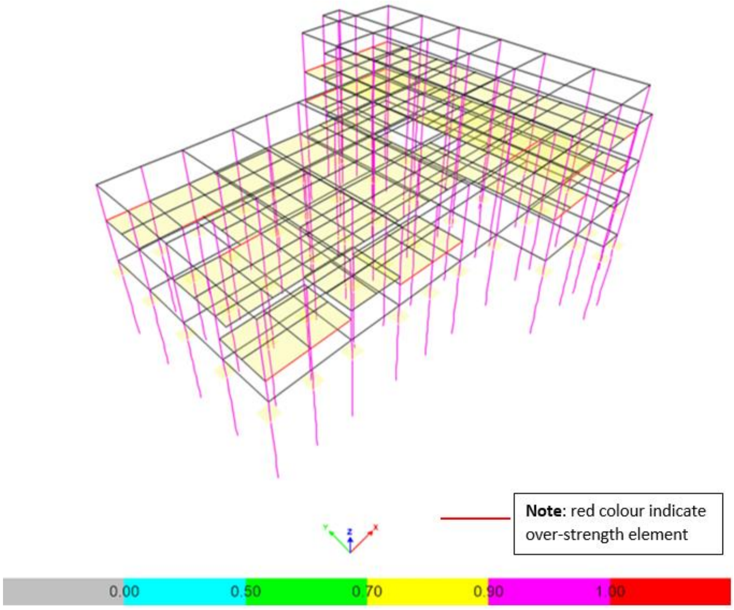

Fig. 12. Stress ratio of a concrete structure after earthquake loading

Figure 13 presents a diagram of the distribution of internal forces in structural elements under the combined support of loads. Figures 13a-c show the internal force distribution for the bending moment diagram (BMD), shear force diagram (SFD), and normal force diagram (NFD), respectively. Table 5 shows the force values in the structure before and after earthquake loading. The analysis results show that applying earthquake loads produces forces in the structure that are more significant than the internal forces that occur without earthquake loads. The finite element analysis results indicate that all column types are safe and do not experience excessive pressure. However, there is a decrease in structural strength in beams of types B1, B2, and B5 that exhibit structural weakening elements. A weakness in the beam prevents the element from withstanding shear loads during earthquakes.

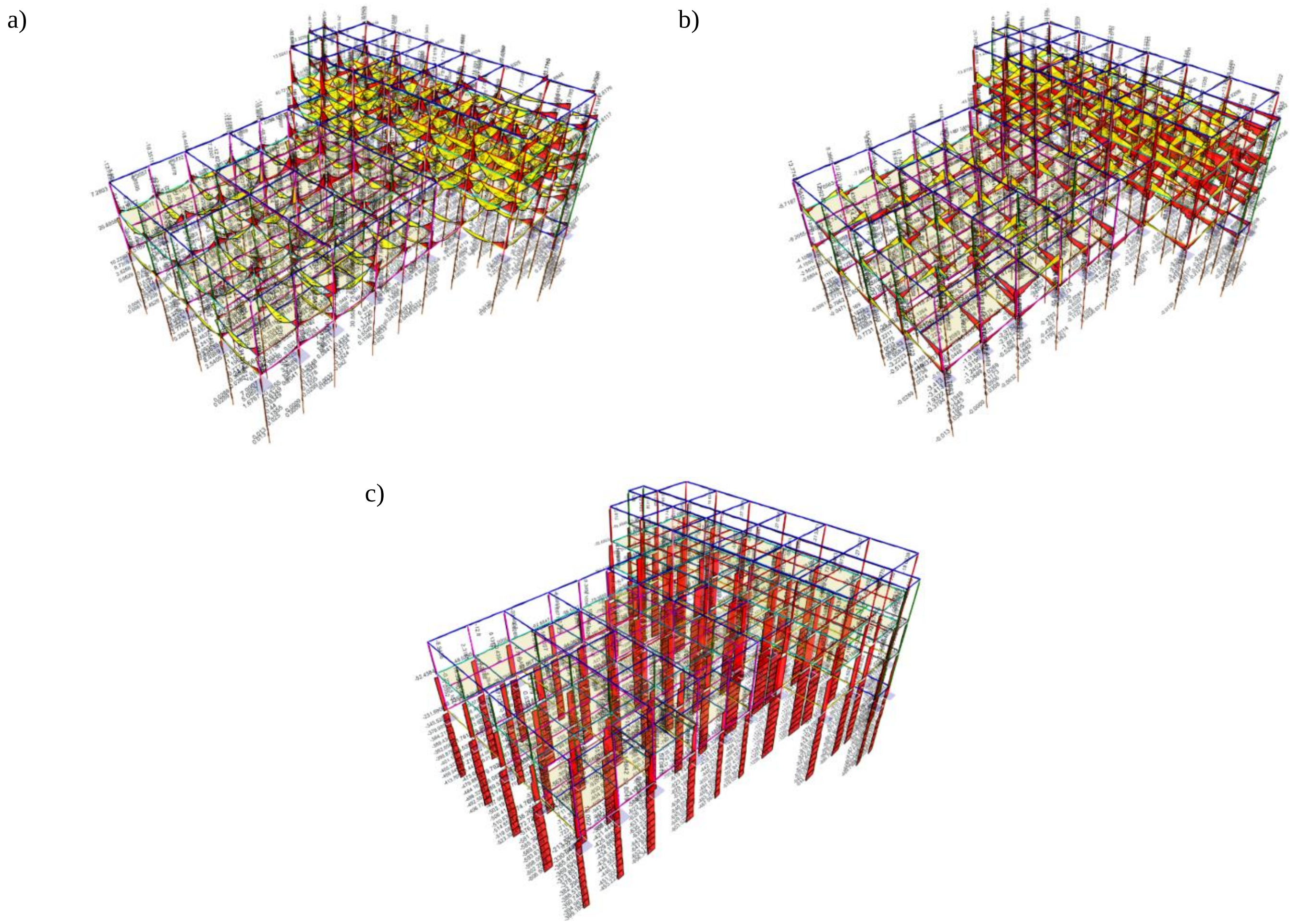

Fig. 13. Internal force diagram (a) BMD, (b) SFD, and (c) NFD

3.6. Concern about the retrofitting method to improve weak element performance

The analysis results show that some beams require special strengthening against shear loads. Several beams appear to be shear-overloaded, meaning they cannot withstand shear loads during an earthquake. One way to improve beam performance is to retrofit or strengthen the structure [55]. The retrofitting method involves adding new structural elements to existing building systems to prevent earthquake damage [56]. One of the strengthening methods used is concrete jacketing. This process involves adding a new layer of concrete to the existing beam's surface and installing additional flexural and shear reinforcement to improve the beam's performance. Increasing the beam's dimensions significantly affects its stiffness. Increasing the beam's width and height plays an important role in determining the beam's stiffness against bending forces. The wider the beam, the greater its bending stiffness. This is because the beam's width affects the beam's moment of inertia [57].

The cross-section of a beam experiencing weakening is shown in Fig. 14. Modelling of beam strengthening with concrete jacketing is shown in Fig. 15. In this study, strengthening was carried out only by adding a minimum layer of concrete and reinforcement. The increases in cross-sectional area and number of reinforcements before and after concrete jacketing were 52% for type B1 beams, 47% for type B2, and 53% for type B5. The reinforcement added in retrofitting is modelled using the amount of reinforcement as in the beam field. This is conducted so that the beam's load can be applied at least once before weakening occurs. Concrete jacketing analysis involves evaluating the structure to be reinforced using additional layers of concrete [58-60]. However, in this study, a more specific analysis, such as an experimental analysis, was not conducted to strengthen the concrete jacketing. It can be presented in further study. However, in this study, the perspective on the feasibility of retrofit solutions through reinforcement was limited to adding only the minimum concrete blanket and reinforcement, which could provide structural improvements to help protect the structure against earthquake impacts.

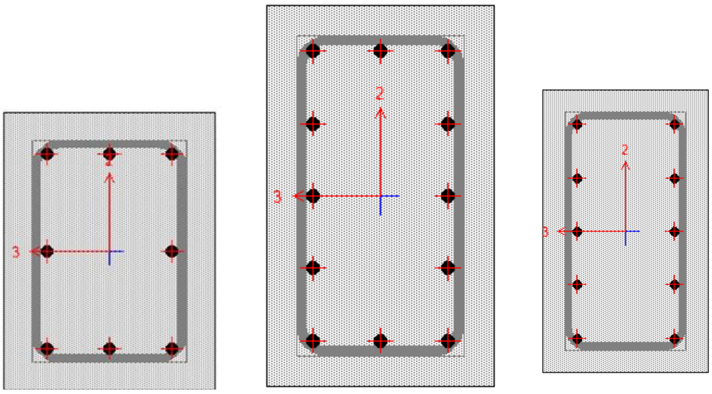

a) b) c)

Fig. 14. Beam cross-sections before concrete jacketing for (a) B1, (b) B2, and (c) B5

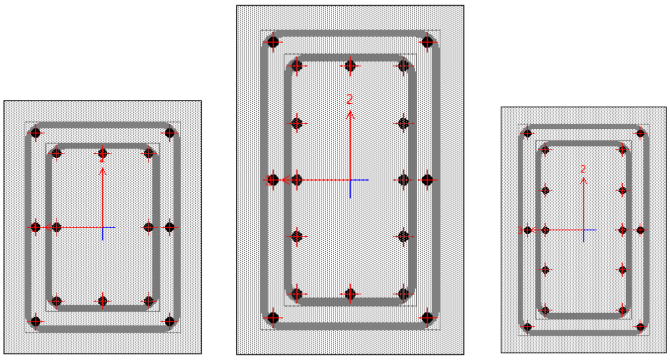

a) b) c)

Fig. 15. Beam cross-sections after concrete jacketing for (a) B1, (b) B2, and (c) B5

After strengthening is complete and a re-inspection is carried out, the structure has been effectively strengthened, and no beam or column elements exhibit weakness or over-strength, as indicated in red. Figure 16 presents the distribution of internal forces in structural elements after retrofitting, whereas Fig. 17 shows no indications of weak elements. This indicates that the retrofitting method of concrete jacketing could be numerically confirmed as an alternative to improve the structure's performance.

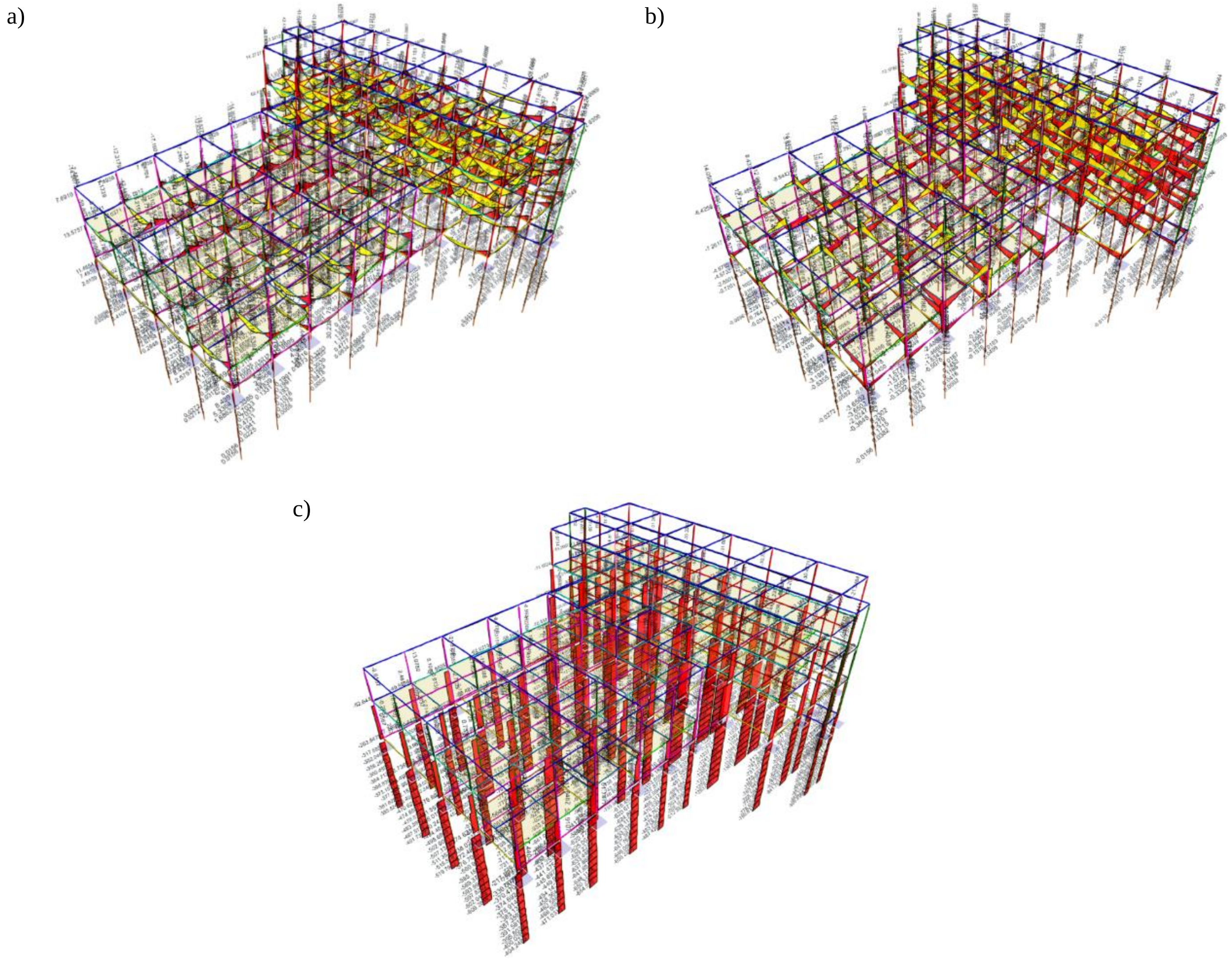

Fig. 16. Internal force diagram after concrete jacketing for (a) BMD, (b) SFD, and (c) NFD

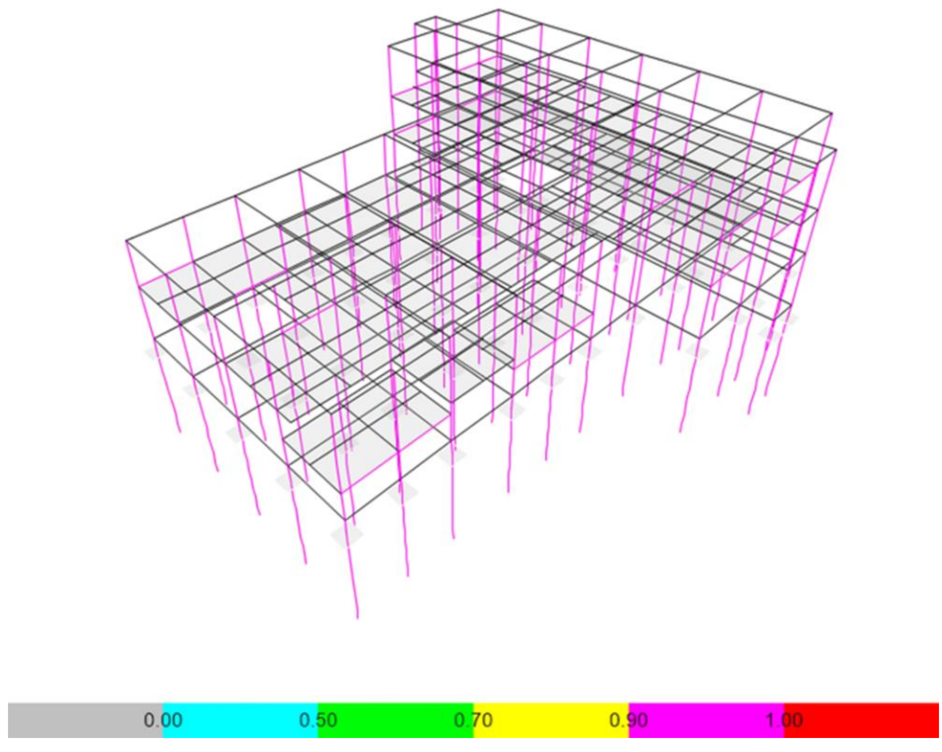

Fig. 17. Stress ratio of the concrete structure after earthquake loading

4. Conclusion

This paper presents a coupling of ground response and structural dynamic analyses to assess the building performance of the Moot Court Building at the University of Bengkulu, Indonesia. The site investigation is performed. Furthermore, a one-dimensional seismic ground-response analysis is performed to obtain soil-structure interaction parameters. Structural dynamic analysis is performed to inspect building performance. The numerical analysis of the retrofitting method is also presented. Several concluding remarks can be drawn:

1. Seismic response analysis obtained a maximum PGA value of 0.259 g. The study area experienced a 1.684 amplification in the surface soil layer. This causes the wave to propagate to the surface and amplify. The role of a weak layer near the surface could amplify the seismic motion at the ground surface.
2. The intensity parameter reflects the potential seismic damage. The site is predicted to undergo amplification at the ground surface. Therefore, ground motion at the surface is generally higher and exhibits the highest intensity parameters during seismic wave propagation. To minimise the potential seismic damage, soil improvement is important. It can improve soil resistance and damping, thereby minimising amplification during seismic wave propagation.
3. Time history analysis of structural dynamic analysis considering ground motion at the pile tip layer shows that structural elements experiencing weakening occur at the edges of the building. The elements experiencing weakening are beams of types B1, B2, and B5, with percentage increases in overstrength of 61%, 100%, and 80%, respectively. This is also caused by reduced restraining force at the edge of the building compared to the centre.
4. Based on the weakening, retrofitting uses the concrete jacketing method to increase the cross-sectional area and reinforce the weakened elements. The increase in the cross-sectional area of beam types B1, B2, and B3 is 52%, 47%, and 53%, respectively, of the previous element's cross-sectional area.
5. The implementation of coupling analysis based on seismic ground response and structural dynamic analysis for building assessment is introduced in this study. This study's framework can be implemented to inspect other buildings in other areas. However, the limited reliability of the retrofit solution due to the updated seismic design code remains an issue. Therefore, it is important to perform an experimental study to model it. It will be presented in further studies.

References

[1] Mase L.Z., Local seismic hazard map based on the response spectra of stiff and very dense soils in Bengkulu city, Indonesia, *Geodesy and Geodynamics* 13(6) (2022) 573–584. https://doi.org/10.1016/j.geog.2022.05.003

[2] Misliniyati R., Mase L.Z., Syahbana A.J., Soebowo E., Seismic hazard mitigation for Bengkulu Coastal area based on site class analysis, *IOP Conference Series: Earth and Environmental Science* 212(1) (2018) 012004. https://doi.org/10.1088/1755-1315/212/1/012004

[3] Mase L.Z., Sugianto N., Refrizon, Seismic hazard microzonation of Bengkulu City, Indonesia, *Geoenvironmental Disasters* 8(1) (2021) 5. https://doi.org/10.1186/s40677-021-00178-y

[4] Mase L.Z., Refrizon, Rosiana, Anggraini P.W., Local Site Investigation and Ground Response Analysis on Downstream Area of Muara Bangkahulu River, Bengkulu City, Indonesia, *Indian Geotechnical Journal* 51(5) (2021) 952–966 . https://doi.org/10.1007/s40098-020-00480-w

[5] Mase L.Z., Seismic Hazard Vulnerability of Bengkulu City, Indonesia, Based on Deterministic Seismic Hazard Analysis, *Geotechnical and Geological Engineering* 38(5) (2020) 5433–5455. https://doi.org/10.1007/s10706-020-01375-6

[6] Mase L.Z., Reliability study of spectral acceleration designs against earthquakes in Bengkulu City, Indonesia, *International Journal of Technology* 9(5) (2018) 910–924. https://doi.org/10.14716/ijtech.v9i5.621

[7] Sun C.G., Cho H.I., Kim H.S., Kim D.S., Assessment of new Korean site classification and design response spectra, *Géotechnique Letters* 8(1) (2018) 25–31. https://doi.org/10.1680/jgele.17.00108

[8] Yoshida N., Seismic Ground Response Analysis, *Springer Netherlands* (2015). https://doi.org/10.1007/978-94-017-9460-2

[9] Qodri M.F., Mase L.Z., Likitlersuang S., Non-linear site response analysis of bangkok subsoils due to earthquakes triggered by three pagodas fault, *Engineering Journal* 25(1) (2021) 43–52. https://doi.org/10.4186/ej.2021.25.1.43

[10] Tabatabaiefar S.H.R., Fatahi B., Samali B., Seismic Behavior of Building Frames Considering Dynamic Soil-Structure Interaction, *International Journal of Geomechanics* 13(4) (2013) 409–420. https://doi.org/10.1061/(ASCE)GM.1943-5622.0000231

[11] Dutta S.C., Bhattacharya K., Roy R., Response of low-rise buildings under seismic ground excitation incorporating soil–structure interaction, Soil Dynamics and Earthquake Engineering 24(12) (2004) 893–914. https://doi.org/10.1016/J.SOILDYN.2004.07.001

[12] Jiang J., El Nggar H.M., Xu C., Zhong Z., Du X., Effect of ground motion characteristics on seismic fragility of subway station, Soil Dynamics and Earthquake Engineering 143 (2021) 106618. https://doi.org/10.1016/j.soildyn.2021.106618

[13] Standardisation Council of Indonesia, *SNI 1726:2019, Procedures for Earthquake Resistance Planning for Building and Non-Building Structures*, Jakarta, 2019.

[14] Standardisation Council of Indonesia, *SNI 1726:2012 Procedures for Earthquake Resistance Planning for Building and Non-Building Structures*, Jakarta, 2012.

[15] Zhang X.R., et al., Late Eocene subduction initiation of the Indian Ocean in the North Sulawesi Arc, Indonesia, induced by abrupt Australian plate acceleration, *Lithos* 422–423 (2022) 106742. https://doi.org/10.1016/J.LITHOS.2022.106742

[16] Sieh K., Natawidjaja D., Neotectonics of the Sumatran fault, Indonesia, *Journal of Geophysical Research: Solid Earth* 105(B12) (2000) 28295–28326. https://doi.org/10.1029/2000JB900120

[17] Pararas-Carayannis G., Brief History of Early Pioneering Tsunami Research – Part A, *Science of Tsunami Hazards* 37(1) (2018) 49.

[18] Mase L.Z., Irsyam M., Gustiparani D., Noptapia A.N., Syahbana A.J., Soebowo E., Identification of bedrock depth along a downstream segment of Muara Bangkahulu River, Bengkulu City, Indonesia, *Bulletin of Engineering Geology and the Environment* 83(4) (2024) 93. https://doi.org/10.1007/s10064-024-03591-3

[19] Mukti M.M., Maulin H.B., Permana H., Growth of forearc highs and basins in the oblique Sumatra subduction system, *Petroleum Exploration and Development* 48(3) (2021) 683–692. https://doi.org/10.1016/S1876-3804(21)60054-X

[20] Jacob J., Dyment J., Ghosal D., Dewangan P., Strike-slip seismicity at the Andaman-Sumatra Subduction Zone: Role of the fracture zones and age of the subducting lithosphere, *Tectonophysics* 811 (2021) 228862. https://doi.org/10.1016/j.tecto.2021.228862

[21] Farid M., Mase L.Z., Implementation of seismic hazard mitigation on the basis of ground shear strain indicator for spatial plan of Bengkulu City, Indonesia, *International Journal of GEOMATE* 18 (2020) 199–207. https://doi.org/10.21660/2020.69.24759

[22] Building Seismic Safety Council, *NEHRP Recommended Seismic Provisions for New Buildings and Other Structures (FEMA P-2082-1)*, Washington, D.C., 2020.

[23] Hollender F., et al., Characterization of site conditions (soil class, VS30, velocity profiles) for 33 stations from the French permanent accelerometric network (RAP) using surface-wave methods, *Bulletin of Earthquake Engineering* 16(6) (2018) 2337–2365. https://doi.org/10.1007/s10518-017-0135-5

[24] Hausler E., Anderson A., *Observation of the 12 and 13 September 2007 Earthquake, Sumatra, Indonesia*, Build Change, Colorado, 2007. [Online]. Available: https://buildchangeweb.s3.amazonaws.com/resources/tech/BC_Bengkulu_English.pdf

[25] Miller R.D., Xia J., Park C.B., Ivanov J., Williams E., Using MASW to map bedrock in Olathe, Kansas, in *SEG Technical Program Expanded Abstracts*, Society of Exploration Geophysicists (1999) 433–436. https://doi.org/10.1190/1.1821045

[26] Viani M.L., *Bedrock Depth Mapping Using Shear Wave Velocity in Muara Bangkaulu District*, Indonesia, 2021.

[27] Mase L.Z., Liquefaction potential analysis along coastal area of Bengkulu Province due to the 2007 Mw 8.6 Bengkulu earthquake, *Journal of Engineering and Technological Sciences* 49(6) (2017) 721–736. https://doi.org/10.5614/j.eng.technol.sci.2017.49.6.2

[28] Travasarou T., Bray J.D., Abrahamson N.A., Empirical attenuation relationship for Arias intensity, *Earthquake Engineering & Structural Dynamics* 32(7) (2003) 1133–1155. https://doi.org/10.1002/eqe.270

[29] Campbell K.W., Bozorgnia Y., A comparison of ground motion prediction equations for Arias intensity and cumulative absolute velocity developed using a consistent database and functional form, *Earthquake Spectra* 28(3) (2012) 931–941. https://doi.org/10.1193/1.4000067

[30] Elhout E.A., The correlation between the ground motion intensity measure parameters of earthquakes, *Asian Journal of Civil Engineering* 21(5) (2020) 829–840. https://doi.org/10.1007/s42107-020-00243-1

[31] Gogoi A., Baruah S., Sharma S., Regression analysis on ground motion parameters for the earthquakes (Mw ≥ 4.0) in Northeast India with special emphasis on 3 January 2016 Mw 6.7 Tamenglong earthquake, *Physics and Chemistry of the Earth, Parts A/B/C* 129 (2023) 103316. https://doi.org/10.1016/j.pce.2022.103316

[32] Malhotra P.K., Cyclic-demand spectrum, *Earthquake Engineering & Structural Dynamics* 31 (2002) 1441–1457. https://doi.org/10.1002/eqe.171

[33] Hancock J., Bommer J.J., The effective number of cycles of earthquake ground motion, *Earthquake Engineering & Structural Dynamics* 34 (2005) 637–664. https://doi.org/10.1002/eqe.437

[34] Panella D.S., Tornello M.E., Frau C.D., A simple and intuitive procedure to identify pulse-like ground motions, *Soil Dynamics and Earthquake Engineering* 94 (2017) 234–243. https://doi.org/10.1016/j.soildyn.2017.01.020

[35] Mase L.Z., Yundrismein R., Nursalam M.A., Putra S.M., Shelina A., Nugroho S.H., A study of building performance inspection based on a combination of site-specific response analysis and structural analysis (A case study of the Lighthouse View Tower in Bengkulu City, Indonesia), *Rudarsko Geolosko Naftni Zbornik* 37(3) (2022) 197–209. https://doi.org/10.17794/rgn.2022.3.14

[36] Fener M., Kahraman S., Bay Y., Gunaydin O., Correlations between P-wave velocity and Atterberg limits of cohesive soils, *Canadian Geotechnical Journal* 42(2) (2005) 673–677. https://doi.org/10.1139/t04-102

[37] Hashash Y.M.A., Park D., Viscous damping formulation and high frequency motion propagation in non-linear site response analysis, *Soil Dynamics and Earthquake Engineering* 22(7) (2002) 611–624. https://doi.org/10.1016/S0267-7261(02)00042-8

[38] Misliniyati R., Mase L.Z., Irsyam M., Hendriawan H., Sahadewa A., Seismic response validation of simulated soil models to vertical array record during a strong earthquake, *Journal of Engineering and Technological Sciences* 51(6) (2019) 772–790. https://doi.org/10.5614/j.eng.technol.sci.2019.51.6.3

[39] Mahmood K., Rehman Z.ur., Farooq K., Memon S.A., One dimensional equivalent linear ground response analysis — A case study of collapsed Margalla Tower in Islamabad during 2005 Muzaffarabad earthquake, *Journal of Applied Geophysics* 130 (2016) 110–117. https://doi.org/10.1016/j.jappgeo.2016.04.015

[40] Hashash Y.M., Musgrove M.I., Harmon J.A., Groholski D.R., Phillips C.A., Park D., *Nonlinear and Equivalent Linear Seismic Site Response of One-Dimensional Soil Columns Version 7.1*, University of Illinois at Urbana-Champaign (2020).

[41] Vucetic M., Dobry R., Effect of soil plasticity on cyclic response, *Journal of Geotechnical Engineering* 117(1) (1991) 89–107. https://doi.org/10.1061/(ASCE)0733-9410(1991)117:1(89)

[42] Seed H.B., Idriss I.M., *Soil Moduli and Damping Factors for Dynamic Response Analysis*, Earthquake Engineering Research Center, University of California, Berkeley, California, 1970.

[43] Standardisation Council of Indonesia, *SNI 1727:2013, Minimum Loads for Planning Buildings and Other Structures*, Jakarta, 2013.

[44] Bowles J.E., *Foundation Analysis and Design*, 5th ed. New York: McGraw-Hill, 1997.

[45] Aoki N., Velloso D.D.A., An approximate method to estimate the bearing capacity of piles, in *Proceedings of the 5th Pan-American Conference of Soil Mechanics and Foundation Engineering*, International Society of Soil Mechanics and Geotechnical Engineering, Buenos Aires (1975) 367–376.

[46] Habib A., Yildirim U., Eren O., Column repair and strengthening using RC jacketing: a brief state-of-the-art review, *Innovative Infrastructure Solutions* 5(3) (2020) 75. https://doi.org/10.1007/s41062-020-00329-4

[47] Hong S.G., Lee J.H., Choi Y., Gu I.Y., Seismic strengthening of concrete columns by ultrahigh-performance fiber-reinforced concrete jacketing, *Journal of Structural Engineering* 147(10) (2021) 04021157. https://doi.org/10.1061/(ASCE)ST.1943-541X.0003111

[48] Finn W.D.L., Ruz F., Amplification effects of thin soft-surface layers, *Earthquake Spectra* 32(4) (2016) 2109–2126. https://doi.org/10.1193/101914EQS164M

[49] Mase L.Z., Likitlersuang S., Tobita T., Analysis of seismic ground response caused during strong earthquake in Northern Thailand, *Soil Dynamics and Earthquake Engineering* 114 (2018) 113–126. https://doi.org/10.1016/J.SOILDYN.2018.07.006

[50] Kobayashi H., Koketsu K., Miyake H., Rupture processes of the 2016 Kumamoto earthquake sequence: Causes for extreme ground motions, *Geophysical Research Letters* 44(12) (2017) 6002–6010. https://doi.org/10.1002/2017GL073857

[51] Reis C., Lopes M., Baptista M.A., Clain S., Towards an integrated framework for the risk assessment of coastal structures exposed to earthquake and tsunami hazards, *Resilient Cities and Structures* 1(2) (2022) 57–75. https://doi.org/10.1016/j.rcns.2022.07.001

[52] Nardo A., Biondi G., Casablanca O., Di Filippo G., Cascone E., Seismic intensity measures and predictive equations for the evaluation of earthquake-induced crest settlements of earth dams, *Earthquake Engineering & Structural Dynamics* 53(9) (2024) 2680–2709. https://doi.org/10.1002/eqe.4135

[53] Mase L.Z., Likitlersuang S., Tobita T., Ground motion parameters and resonance effect during strong earthquake in Northern Thailand, *Geotechnical and Geological Engineering* 39(3) (2021) 2207–2219. https://doi.org/10.1007/s10706-020-01619-5

[54] El-Maissi A.M., Kassem M.M., Tan C.G., Fikri R., Nazri F.M., Damage index seismic assessment methodologies of URM buildings: a state-of-the-art review, *Engineering Journal* 26(1) (2022) 39–53. https://doi.org/10.4186/ej.2022.26.1.39

[55] Kazem Sharbatdar M., Kheyroddin A., Emami E., Cyclic performance of retrofitted reinforced concrete beam–column joints using steel prop, *Construction and Building Materials* 36 (2012) 287–294. https://doi.org/10.1016/j.conbuildmat.2012.04.115

[56] Bhattacharya S., Nayak S., Dutta S.C., A critical review of retrofitting methods for unreinforced masonry structures, *International Journal of Disaster Risk Reduction* 7 (2014) 51–67. https://doi.org/10.1016/j.ijdrr.2013.12.004

[57] Mohammadhassani M., Bin Jumaat M.Z., Chemrouk M., Maghsoudi A.A., Jameel M., Akib S., An experimental investigation on bending stiffness and neutral axis depth variation of over-reinforced high strength concrete beams, *Nuclear Engineering and Design* 241(6) (2011) 2060–2067. https://doi.org/10.1016/j.nucengdes.2011.02.022

[58] Alhadid M.M.A., Youssef M.A., Analysis of reinforced concrete beams strengthened using concrete jackets, *Engineering Structures* 132 (2017) 172–187. https://doi.org/10.1016/j.engstruct.2016.11.014

[59] Mase L.Z., Likitlersuang S., Tobita T., Non-linear site response analysis of soil sites in Northern Thailand during the Mw 6.8 Tarlay earthquake, *Engineering Journal* 22(3) (2018) 291–303. https://doi.org/10.4186/ej.2018.22.3.291

[60] Tanapalungkorn W., Mase L.Z., Latcharote P., Likitlersuang S., Verification of attenuation models based on strong ground motion data in Northern Thailand, *Soil Dynamics and Earthquake Engineering* 133 (2020) 106145. https://doi.org/10.1016/j.soildyn.2020.106145

[61] Mase L.Z., Tanapalungkorn W., Ueda K., Likitlersuang S., Non-linear site response analysis of liquefaction in the port area of Bengkulu City due to large subduction earthquakes, *Transportation Infrastructure Geotechnology* 12(2) (2025) 87. https://doi.org/10.1007/S40515-025-00540-9

[62] Mase L.Z., Tanapalungkorn W., Likitlersuang S., Ueda K., Tobita T., Ground motion, liquefaction and hazard analysis at the Palu site during the 2018 Indonesian great earthquake (Mw 7.5). China Geology 9(1) (2026) 152-174. https://doi.org/10.31035/cg2024067

[63] Julyani V., Mase L.Z., Hardiansyah H., Misliniyati R., Amri K., Likitlersuang S., A case study on geophysical characterisation of bedrock depth and soil stratigraphy, *Transportation Infrastructure Geotechnology* 12(6) (2025) 173. https://doi.org/10.1007/S40515-025-00627-3

[64] Mase L.Z., Tanapalungkorn W., Anussornrajkit P., Likitlersuang S., Assessing liquefaction risk and hazard mapping in a high-seismic region: a case study of Bengkulu City, Indonesia, *Natural Hazards* 121 (2025) 6597–6623. https://doi.org/10.1007/S11069-024-07057-3

[65] Adrian M.N., et al., A case study of soil resistance microzonation based on shear wave velocity, *Transportation Infrastructure Geotechnology* 12(5) (2025) 136. https://doi.org/10.1007/S40515-025-00595-8

[66] Mase L.Z., Likitlersuang S., Tobita T., Chaiprakaikeow S., Soralump S., Local site investigation of liquefied soils caused by earthquake in Northern Thailand, *Journal of Earthquake Engineering* 24(7) (2020) 1181–1204. https://doi.org/10.1080/13632469.2018.1469441

[67] Mase L.Z., Likitlersuang S., Tobita T., Verification of liquefaction potential during the strong earthquake at the border of Thailand-Myanmar, *Journal of Earthquake Engineering* 26(4) (2022) 2023–2050. https://doi.org/10.1080/13632469.2020.1751346

[68] Mase L.Z., Likitlersuang S., Tobita T., Cyclic behaviour and liquefaction resistance of Izumio sands in Osaka, Japan, *Marine Georesources & Geotechnology* 37(7) (2019) 765–774. https://doi.org/10.1080/1064119X.2018.1485793

[69] Mase L.Z., et al., Application of simplified energy concept for liquefaction prediction in Bengkulu City, Indonesia, *Geotechnical and Geological Engineering* 41 (2023) 1999–2021. https://doi.org/10.1007/S10706-023-02388-7